TNFα increases Tyrosine Hydroxylase expression in human monocytes

Adithya Gopinath*[a1], Martin Badov[a1], Madison Francis[a1], Gerry Shaw[1,2], Anthony Collins[1], Douglas R. Miller[1], Carissa A. Hansen[1], Phillip Mackie[1], Malú Gámez Tansey[1], Abeer Dagra[1], Irina Madorsky[2], Adolfo Ramirez-Zamora[3], Michael S. Okun[1,3], Wolfgang J. Streit[1], Habibeh Khoshbouei[1]

1-University of Florida, Department of Neuroscience, Center for Translational Research in Neurodegenerative Disease, Norman Fixel Institute for Neurological Diseases

2-Encor Biotechnology Inc. 4949 SW 41st Blvd Suite 40, Gainesville FL 32608

3-University of Florida, Department of Neurology

[a] equal contribution

Corresponding Author:

*Adithya Gopinath

adithya@ufl.edu

Number of Tables: 4

Number of Figures: 7

Number of Supplemental Figures/Tables: 3

Number of References: 92

Abbreviations: No non-standard abbreviations used

Abstract

Most, if not all, peripheral immune cells in humans and animals express tyrosine hydroxylase (TH), the rate limiting enzyme in catecholamine synthesis. Since TH is typically studied in the context of brain catecholamine signaling, little is known about changes in TH production and function in peripheral immune cells. This knowledge gap is due, in part, to the lack of an adequately sensitive assay to measure TH in immune cells expressing lower TH levels compared to other TH expressing cells. Here, we report the development of a highly sensitive and reproducible Bio-ELISA to quantify picogram levels of TH in multiple model systems. We have applied this assay to monocytes isolated from blood of persons with Parkinson's disease (PD) and to age-matched, healthy controls. Our study unexpectedly revealed that PD patients' monocytes express significantly higher levels of TH protein in peripheral monocytes relative to healthy controls. Tumor necrosis factor (TNFα), a pro-inflammatory cytokine, has also been shown to be increased in the brains and peripheral circulation in human PD, as well as in animal models of PD. Therefore, we investigated a possible connection between higher levels of TH protein and the known increase in circulating TNFα in PD. Monocytes isolated from healthy donors were treated with TNFα or with TNFα in the presence of an inhibitor. Tissue plasminogen activator (TPA) was used as a positive control. We observed that TNFα stimulation increased both the number of TH+ monocytes and the quantity of TH per monocyte, without increasing the total numbers of monocytes. These results revealed that TNFα could potentially modify monocytic TH production and serve a regulatory role in peripheral immune function. The development and application of a highly sensitive assay to quantify TH in both human and animal cells will provide a novel tool for further investigating possible PD immune regulatory pathways between brain and periphery.

Introduction

Human and animal studies have shown that most if not all immune cells possess components necessary to release, uptake, synthesize, and respond to catecholamines including dopamine and norepinephrine (NOR). These components activate signaling cascades that change the phenotype and function of cells in both healthy and in disease conditions. Immune cells may thus both come in contact with physiological levels of catecholamines derived from peripheral tissues and also serve as a source for catecholamines. Tyrosine hydroxylase (TH) catalyzes the conversion of tyrosine to 3,4-dihydroxyphenylalanine (L-DOPA), which is the rate-limiting step in the synthesis of dopamine, norepinephrine (NOR) and epinephrine[1,2]. Although primarily studied in the central nervous system[3,4], TH is expressed in the majority of peripheral immune cells[5-9], and many peripheral tissues[10], including kidney[11,12], heart[13] and adrenal cortex[14-16]. Both myeloid and lymphoid lineages of human peripheral immune cells express TH[17,18], which is thought to regulate dopamine levels within these cells[9]. Beyond protein expression, TH activity is regulated by a variety of post-translational modifications and that can regulate TH function. For example, phosphorylation, ubiquitination, nitration and S-glutathionlyation can all affect TH activity independent of TH levels[19-26]. As the key to catecholamine production, TH activity and its relative expression are commonly studied in diseases in which catecholamine tone, synthesis and signaling are altered. These disease states include bipolar disorder, addiction, schizophrenia, attention deficit hyperactivity (ADHD) and neurodegenerative conditions including Parkinson's disease (PD).

The lack of a robust and sensitive assay to measure low levels of TH protein has hampered the field's ability to investigate TH protein levels in peripheral immune cells in diseases characterized by altered catecholamine tone. For example, in PD, due to its spatially restricted expression, decreases in TH levels in the basal ganglia are readily detectable[27,28], whereas changes in TH levels in other brain regions (i.e., amygdala, hippocampus, cortical regions) are reported in the later stages of PD[29,30]. In contrast, very low TH levels in countless immune cells spread across the body has made it difficult to study TH protein levels in

peripheral immune cells. For example, indirect TH measurements via qPCR reveal that PD patients show significantly less midbrain TH mRNA compared to healthy controls subjects (5.5 ± 1.4 in healthy controls, vs. 1.5 ± 0.9 attomole/microgram total RNA in PD)[31]. In contrast, TH mRNA is not detectable in unstimulated immune cells[32]. TH protein expression in the substantia nigra is in excess of 200ng TH per milligram protein[33], and is decreased in patients with PD. However, to our knowledge no reports directly quantify TH protein in immune cells.

In order to investigate whether the characteristically reduced TH expression in PD central nervous system (CNS) is recapitulated in peripheral immune cells, we established a sensitive assay to quantify TH protein. We then applied the assay to analyze TH production in peripheral blood monocytes. The sensitivity of our Bio-ELISA was a thousand-fold above traditional detection methods, and when we measured TH level in peripheral monocytes from healthy controls and from PD, we observed a significant elevation of TH levels in PD monocytes versus controls. This observation was contrary to our *a priori* hypothesis. The unexpected discovery of increased TH protein in peripheral PD monocytes prompted investigation into the potential underlying mechanism. In the PD literature, there is a strong consensus that neuroinflammatory cytokines, including TNFα and IL6 are increased in CSF and serum of PD patients and of animal models of PD[27,34-42]. Therefore, we investigated whether *ex vivo* exposure to TNFα or IL6 increases the number of TH+ monocytes and/or amount of TH protein per monocyte. We found that exposure to TNFα, but not IL6 increased both the number of TH+ monocytes and the quantity of TH protein per cell.

Results and discussion

Bio-ELISA successfully and reproducibly detects recombinant and native TH.

To test the hypothesis that similar to CNS in PD, TH expression is reduced in peripheral blood monocytes, we first established a sensitive assay to quantify TH levels in monocytes from healthy controls, as well as various reference TH expressing systems. Given the plethora of

biological systems expressing TH, there is an unmet need for a sensitive and reliable assay to quantify TH levels which with broad biological implications in basic science, preclinical and clinical research. To date, measurement of TH levels in midbrain neurons has been accomplished by immunohistochemistry, and Western blot[62-65], while TH levels in peripheral immune cells has been assayed by flow cytometry[51]. Although reliable, these methods share a common shortcoming in that they are semi-quantitative at best, and at worst only indicate the presence or absence of TH. This led us to develop a highly sensitive and fully quantitative enzyme-linked immunosorbent assay (Bio-ELISA) to measure TH protein levels.

Quantification of TH using Bio-ELISA depends on the availability of purified TH and high-quality antibodies against TH, preferably generated in two distinct host species. A panel of monoclonal and polyclonal antibodies were generated against full length recombinant human TH (Figure 1A), and quality assessment was performed by standard ELISA, Western blotting, and appropriate cell and tissue staining. These novel antibodies behaved in all respects similarly to a widely used commercial TH antibody (Figure 1B, AB152, Millipore-Sigma)[66-69]. A mouse monoclonal antibody, MCA-4H2, and a rabbit polyclonal, RPCA-TH, were selected as ELISA capture and detection antibodies, respectively.

Next, TH recombinant protein band identity was compared to TH expression in PC12 cells (Figure 1C). As predicted, PC12 lysate shows a single TH band at ~63 kDa, with a corresponding band for the TH recombinant protein at ~70 kDa. The observed difference in molecular weight between TH expressed in PC12 cells and recombinant TH protein is due to the additional 5.7kDa N-terminal His-tag. Lower molecular weight bands (at 50kDa and 35kDA, Figure 1B-E, Supplementary Figure 1) represent proteolytic cleavage products of mammalian TH when expressed in a prokaryotic system. Both MCA-4H2 and RPCA-TH reliably detect both recombinant TH and native TH in PC12 lysates (Figure 1 C, D).

Since antibody specificity is crucial for developing a novel assay, we rigorously confirmed their specificity. First, MCA-4H2 and RPCA-TH were used to stain human and murine

midbrain tissue (Figure 2). MCA-4H2 (Figure 2A) and RPCA-TH (Figure 2B) both showed high specificity for TH+ dopamine neurons in both human and murine tissues with no visible background. In addition, both secondary-only and isotype control staining show minimal background (Figure 2A-B, top and second panels). Lastly, both MCA-4H2 and RPCA-TH were tested via Western blot using standard immunoblotting as well as blocking peptide/absorption controls (Figure 2C-D). Both antibodies show good specificity and minimal background. CHO cells, used as the negative control since they do not express TH, show no TH band (Figure 2C). The peptide blocking/absorption control groups (Figure 2D) also show no detectable signal, further confirming specificity.

Next, we prepared 1:1 serial dilutions of TH recombinant protein in Laemmli buffer, from 6ug/mL to 0.094ug/mL, to test the limits of detection using the Licor IR imaging system for Western blot (Figure 1E) using commercially available TH antibody AB152. While effective, detection *via* Licor Odyssey using an IR fluorescent dye affords a fixed lower detection limit of ~15ng, suggesting that IR fluorescent imaging is suitable for high expressing systems, but unsuitable for accurate quantification at low nanogram or picogram TH levels, reinforcing the need for a more sensitive, quantitative TH Bio-ELISA.

To quantify TH expression in control conditions, we first attempted a standard sandwich ELISA approach (Figure 1F), in which MCA-4H2 was used as the capture antibody, followed by incubation with recombinant TH, then RPCA-TH as detection antibody. Enzyme-based detection was accomplished by addition of HRP-conjugated secondary (goat anti-rabbit HRP, Vector, BA1000). While this reliably quantified TH, the standard version of this assay produced a lower detection threshold of 125pg/mL TH. We sought to further increase sensitivity of the assay by addition of a biotin-avidin amplification step (Avidin-HRP, Vector, A2004) (Figure 1G), which provided an improved lower threshold of 62.5pg/mL. A further refinement was the biotinylation of the rabbit detection antibody using Sulfo-NHS-LC-biotin (Thermo Scientific A39257) which improved sensitivity further by reducing background and producing a lower-threshold of

detection at 15pg/mL (Figure 1H) with biotinylated antibodies, hence the Bio-ELISA designation. We found that our Bio-ELISA is around one thousand-fold more sensitive than infrared Western blot imaging (15 pg/mL vs. 15 ng/mL). Both TH antibodies are available commercially from EnCor Biotechnology Inc.

Antibodies MCA-4H2 and RPCA-TH reliably detect both native and denatured TH in mouse and human tissue. Aiming to develop a novel and reliable ELISA for both human and murine tissues, we next sought to confirm specificity of these antibodies on native and denatured tissues from both human and mouse brain regions rich in tyrosine hydroxylase (Figure 2). MCA-4H2 (Figure 2A) and RPCA-TH (Figure 2B) detect TH+ cell bodies and neuronal processes in both human and mouse midbrain. Minimal non-specific staining detected in secondary only and isotype controls, further confirming antibody specificity. Similarly, both MCA-4H2 and RPCA-TH detect denatured TH on Western blot (Figure 2C) following separation on SDS-PAGE, with minimal non-specific bands in the negative control (parental CHO cell homogenate). HSP60 is shown as a loading control. As an additional validation step to confirm the specificity of MCA-4H2 and RPCA-TH, primary antibodies were pre-incubated with recombinant TH protein (blocking peptide/absorption control) and show no observable signal (Figure 2D).

TH Bio-ELISA reliably quantifies TH in PC12 cells, human macrophages, and cultured murine dopamine neurons. Having established a reliable method with a suitably low detection threshold, we tested the TH Bio-ELISA on cell homogenates prepared from PC12 cells, HEK293 cells, cultured primary human macrophages derived from whole blood samples from healthy donors, and primary cultures of midbrain dopamine neurons prepared from PND0-PND3 mouse pups. PC12 cells are known to express high levels of TH[48], while HEK293 serve as negative control[45,70]. Cultured midbrain dopamine neurons are known to express TH as the rate limiting enzyme for dopamine[47] while cultured human monocyte-derived-macrophages express TH protein and mRNA[9,43].

TH expression is shown as unit TH (picogram or nanogram) per mg total protein, as determined by the Lowry assay. PC12 homogenate provided a reliable positive control expressing high levels of TH (>10ng TH/mg total protein), while HEK293 homogenate showed no detectable levels of TH, in at least 6 independent replicates. As anticipated, cultured dopamine neurons from postnatal mice showed greater TH concentrations (~700pg TH/mg total protein) than cultured human macrophages (~300pg TH/mg total protein) (Figure 3A), suggesting the Bio-ELISA is applicable to cell and tissue samples derived from human and murine specimens, paving the way for its application in translational and preclinical studies involving measurements of TH protein. We should note that unlike cultured human monocyte-derived-macrophages, cultured dopamine neurons contain various cell types, and consist of 12-16% dopamine neurons. The remainder are GABAergic neurons and supporting cells (microglia and astroglia)[71-73]. Thus we believe that TH levels are much higher in a single dopamine neuron than in a macrophage. Visual representation of relative TH expression in PC12, HEK293, human macrophage and primary neuron homogenates are plotted on a representative standard curve (Figure 3B). Raw values [TH] in ng/mL calculated from absorbance are shown in Figure 3C, alongside each sample ID. Raw TH concentration was divided by [Protein], then multiplied by 1,000 to produce values in pg TH/mg total protein (Figure 3C).

To further confirm the specificity of these antibodies, the Bio-ELISA was tested using absorption controls (Figure 4). In multiple independent replicates, a single ELISA plate was prepared as shown in Figure 4A (Bio-ELISA, blue; absorbed MCA-4H2, orange; absorbed RPCA-TH, green), and incubated with PC12 lysate as a positive control. Following peptide blocking/absorption of either capture or detection antibody, PC12 cell lysate yields no detectable TH (orange and green arrows, Figure 4B), while the TH Bio-ELISA (blue arrow) recapitulates TH concentrations measured in PC12 cells (compare Figure 3 panel A-B with Figure 4 panel B).

Contrary to our hypothesis, monocytes isolated from blood of PD patients show increased TH protein relative to age-matched healthy controls. PD is a disease in which monoamine signaling is affected in both CNS and peripheral immune cells[9]. The literature supports the hypothesis that similar to the CNS, peripheral TH expression is altered, but there is no reliable information about the direction of this change. Since peripheral immune cells including PBMCs express the machinery for catecholamine synthesis, including TH, they provide a biologically relevant peripheral tissue preparation to investigate TH levels in monocytes of PD patients and age-matched healthy subjects. Monocytes for each subject were isolated from 20 million total peripheral blood mononuclear cells (PBMCs) using anti-CD14 magnetic isolation per manufacturer's instructions. Purified monocytes were immediately lysed and assayed *via* Bio-ELISA for TH concentration following total protein quantification. Of 11 healthy control samples included, only three registered TH concentrations above the detection threshold. By contrast, all 11 PD patients recruited for this study show clear positive TH values that were significantly higher than healthy controls. These data suggest that, contrary to our original hypothesis, PD monocytes express significantly more TH protein relative to healthy control subjects (Fig 5A - n=11, t[20]=3.777, P=0.0012). Mean TH protein concentrations in PD monocytes are shown on a representative standard curve (Figure 5B), along with raw data used to calculate TH concentrations (Figure 5C). While these data represent a snapshot of TH levels in circulation PD monocytes, we cannot make any overarching claims that TH levels in monocytes precede clinical symptoms of PD, or predict a PD diagnosis. A larger sample numbers and longitudinal studies can test these possibilities. Nevertheless, these data suggest that in peripheral monocytes of Parkinson's patients, the rate limiting protein involved in catecholamines synthesis is increased. Investigating the potential mechanism was the focus of the next set of experiments.

TNFα increases number of TH+ monocytes, and the amount of TH protein per monocyte. There is strong evidence in the literature for increased TNFα in PD[27,34-36] including in the brain,

cerebrospinal fluid, and serum of Parkinson's patients[27] as well as in Parkinsonian mice[37,38]. These reports suggest that TNFα plays a role in the often hypothesized peripheral inflammation in PD[74-79], which is also documented in other inflammatory states including rheumatoid arthritis[80,81] and multiple sclerosis[7], where TH expression is linked to TNFα expression[80,81,7]. Therefore, we tested the hypothesis that *ex vivo* stimulation of monocytes from healthy subjects with TNFα stimulates TH expression, as measured by changes in the number of TH-expressing monocytes, and/or the amount of TH per monocyte. We employed flow cytometry to address the former, and bio-ELISA to address the latter. Two million monocytes isolated from whole blood of healthy donors were treated for 4 hours with tissue plasminogen activator (TPA, 100ng/mL, positive control for increased monocyte TH expression[7]), TNFα (17ng/mL)[61] and compared with monocytes treated with vehicle (Figure 6A). Monocytes were assayed for TH expression by two complementary methods: flow cytometry[51] (Figure 6B-F) and ELISA (Figure 6G-H). We should note that because a prolonged TNFα exposure can induce cell toxicity[82-86], we tested multiple treatment durations. We found that a 4-hour TNFα (17ng/mL)[61] treatment had a minimal effect on cell viability; whereas, a longer TNFα exposure substantially decreased cell viability. Therefore, a 4-hour treatment strategy was selected in this study.

To control for donor variability, we added identical quantities of counting beads as a reference. The number of TH+ monocytes was quantified by flow cytometry (Figure 6B, left) in two experimental groups: TPA-treated and TNFα-treated. Monocytes in each condition were gated to isolate single cells expressing TH (Figure 6B). Raw counts of monocytes in each condition revealed increased monocytes expressing TH after treatment with TPA or TNFα (Figure 6D), while the number of TH+ monocytes per microliter (Figure 6C) are significantly increased relative to vehicle (Figure 6E; N=3, $F(2,6)=0.364$, $p=0.0018$), suggesting that the number of TH+ monocytes increase following treatment with TNFα or positive TPA control. A possible mechanism for this observation is either monocyte proliferation during the treatment

period or an altered monocyte phenotype in response to TNFα, with no change in total number of monocytes. In other words, following TNFα treatment, TH+ monocytes may either be increasing in number (proliferation) or existing monocytes upregulate TH expression and become TH+ (phenotypic change). While a four-hour exposure to TNFα is an insufficient time period to induce proliferative events in immune cells[74], we could not confidently rule out these possibilities without additional analyses. Therefore, we quantified monocyte proliferation by comparing the total number of monocytes per microliter of untreated vs. TNFα treated experimental group. We found the total number of monocytes per microliter to be unchanged (Figure 6F). While these results suggest that monocyte proliferation did not occur in response to TNFα, the results of simple cell counts are not definitive. We elected to take a more rigorous approach and assess Ki67 expression as a measure of cell proliferation[87]. Ki67 expression in TNFα treated monocytes relative to vehicle-treated controls revealed no change in Ki67 expression following TNFα treatment (Figure 6I). Thus, these results showed phenotypic changes in monocytes, but not cell proliferation in response to TNFα. While this finding explains our earlier observation of increased numbers of TH+ cells, the potential phenotypic shift following TNFα mediated immune stimulation was an unpredicted and novel finding.

Our flow cytometry data strongly support the conclusion that TNFα increases numbers of TH+ monocytes, but increased number of TH+ monocytes could be due to increased numbers of cells expressing TH protein, increased quantity of TH protein per cell, or both. In order to determine whether or not TNFα treatment increases quantity of TH protein per monocyte, identically treated monocytes were lysed and assayed using our TH Bio-ELISA. We found that four-hour treatments with TNFα significantly increased the amount of TH protein (picogram TH per milligram total protein) above both vehicle and the positive control group (TPA treatment; Figure 6G; n=5-6 per group, $F(2,15)=3.297$, $p=0.0001$), indicating that exposure to TNFα is sufficient to increase TH protein in human monocytes. Overall, our data show that TNFα

increases both the number of monocytes expressing TH and the quantity of TH expressed by each cell.

Inhibition of TNFα blocks increase in number of TH+ monocytes and amount of TH per monocyte. To determine the specificity of TNFα regulation of TH in monocytes, we employed two approaches. We investigated whether inhibition of TNFα signaling attenuates or blocks the TNFα mediated increase in TH. In addition, we asked whether or not interleukin-6 (IL6), a cytokine with pleiotropic effects [71] that is also increased in PD[88-90], and is associated with non-motor symptoms of PD [88-90] can also regulate TH expression in the peripheral monocytes. To test these possibilities, we investigated whether XPro1595, a TNFα inhibitor[91,92], reduces monocyte TH expression relative to TNFα treatment alone. In parallel experiments, monocytes were treated with IL6. Two million monocytes isolated from whole blood of healthy donors (Figure 7A) were treated with XPro1595 alone (50ng/mL), TNFα (17ng/mL) or TNFα plus XPro1595 (Figure 7B), IL6 alone (17ng/mL) or IL6 plus XPro1595. The cells were subjected to flow cytometry or Bio-ELISA. Consistent with the literature [71], we found relative to TNFα treatment alone, XPro1595 inhibition of TNFα reduced both the number of TH+ monocytes and the quantity of TH per monocyte (Figure 7C and D), suggesting that soluble TNFα mediates increased TH in human monocytes. As shown in Figure 7C and 7D, IL6 neither changed the number of TH+ monocytes nor the quantity of TH per monocyte. We should note that our data show that TNFα is capable of regulating TH in monocytes whereas other elevated cytokines, including IL6, are not. Since we have not tested the effect of additional, non-upregulated cytokines, we cannot claim that what we have shown in this study is exclusively mediated by TNFα. Instead, we only claim that TNFα is capable of regulating monocytic TH. In addition, while have not investigated the direct link between increased TH protein in PD monocytes and TNFα, our *ex vivo* data (Figure 6) support the interpretation that TNFα plays a role in increased TH expression in immune cells of PD patients.

In summary, we developed a highly reproducible and quantitative Bio-ELISA to measure TH protein levels in murine and human cells. Following validation of our assay in multiple TH expression systems, we investigated TH expression in PD immune cells and of age-matched healthy control subjects. We observed that PD patients' monocytes expressed significantly greater amounts of TH per monocyte. Inspired by the literature indicating increased TNFα in PD, we uncovered an intriguing link between TNFα stimulation and increased TH expression in healthy monocytes, which is attenuated by treatment with TNFα inhibitor Xpro1595. Given that TH expression and catecholamine release has been shown to be associated with an anti-inflammatory effect and can mitigate TNFα mediated inflammation, we posit that increased TH expression in monocytes in response to elevated TNFα is a compensatory mechanism. This observation is a step towards understanding the potential underlying mechanism and functional consequence of changes in catecholamines in peripheral immune system in PD. Nevertheless, we acknowledge that one of the limitations of this study was the infeasibility of quantifying TNFα responses in PD monocytes. Whereas, TH can be quantified in a 30 mL blood sample (Figures 3-5), for functional assays (Figures 6 and 7) a large blood volume (~500 mL) is required, which is not feasible in PD subjects. In addition, our data represent merely a snapshot of TH levels present in circulating PD monocytes at a single timepoint; we do not make any claims that elevated levels of TH expressing monocytes precede or predict PD. Larger sample numbers and longitudinal studies can test these possibilities. Nonetheless, the current results raise many interesting questions: Do the circulating TH expressing monocytes reflect changes in central dopamine? Does effective PD therapy reduce the level of TH in peripheral immune cells? Does elevated TH in monocytes predict PD onset or its progression? Future studies will examine these questions and the connections between the peripheral immune system to the brain.

Methods

Human subjects: Human brain tissues were obtained *via* approved IRB protocols #IRB201800374 and IRB202002059 respectively. Blood samples were obtained at the University of Florida Center for Movements Disorders and Neurorestoration according to an IRB-approved protocol (#IRB201701195).

Brain tissues from healthy subjects

Human brain tissues were obtained *via* approved IRB protocols IRB202002059 and IRB201800374 , from the UF Neuromedicine Human Brain and Tissue Bank (UF HBTB). The tissues were not associated with identifying information, exempt from consent, therefore no consent was required. Regions of interest were identified and isolated by a board-certified neuropathologist.

Blood samples from healthy subjects

Blood samples from age-matched healthy subjects were obtained from two sources: an approved IRB protocol with written informed consent (IRB201701195), or were purchased from Lifesouth Community Blood Center, Gainesville, FL from August 2017 to January 2020 as deidentified samples, and exempt from informed consent (IRB201700339). According to Lifesouth regulations, healthy donors were individuals aged 50-80 years-old of any gender, who were not known to have any blood borne pathogens (both self-reported and independently verified), and were never diagnosed with a blood disease, such as leukemia or bleeding disorders. In addition, none of the donors were using blood thinners or antibiotics, or were exhibiting signs/symptoms of infectious disease, or had a positive test for viral infection in the previous 21 days.

Blood samples from PD patients:

Blood samples were obtained from PD patients (aged 50-80 years-old of any gender) at the University of Florida Center for Movements Disorders and Neurorestoration according to an IRB-approved protocol (#IRB201701195), via written informed consent. All recruited patients' PD was idiopathic. Patients did not have any recorded blood-borne pathogens or blood

diseases, nor were they currently taking medications for infections according to their medical record. In addition, none of the donors were using blood thinners (warfarin, heparin), antibiotics, over-the-counter (OTC) medications other than aspirin, or were exhibiting signs/symptoms of infectious disease or had a positive test for viral infection in the previous 21 days. Current medications are summarized in Supplementary Table 1.

TH recombinant protein

Full length human TH protein was expressed from a synthetic cDNA inserted into the *EcoRI* and *SalI* sites of the pET30a(+) vector and was codon optimized for expression in *E. coli*. The vector adds an N-terminal His-tag and other vector sequence, a total of 5.7kDa. Expression of the construct was made by standard methods and purification was performed using the His tag by immobilized metal affinity chromatography on a nickel column. The TH sequence used in this study is the human tyrosine 3-monooxygenase isoform shown in Uniprot entry P07101-2.

Model systems used for the validation of bio-ELISA

Human macrophages: Primary human macrophages were cultured as described previously[43]. Peripheral blood mononuclear cells (PBMCs) isolated as described below were re-suspended in RPMI 1640 containing 1% Pen/Strep and 7.5% sterile-filtered, heat-inactivated autologous serum isolated from the donor's own blood, and plated in 24-well untreated polystyrene plates at 1 million PBMCs per well. To retain only monocytes/macrophages, cells were washed after 90 minutes of adherence time to remove non-adherent cells with incomplete RPMI 1640, followed by replacement with complete media. Media was replaced at days 3 and 6 following culture, and cell lysis performed on day 7 following culture.

Primary murine midbrain dopamine neurons: Midbrain dopamine neurons strongly express TH[44] and were used as a positive control group. Acutely dissociated mouse midbrains from 0-2 day-old male and female pups were isolated and incubated in dissociation medium at 37°C under continuous oxygenation for 90 minutes. Dissociated cells were pelleted by centrifugation at 1,500×*g* for 5 min and resuspended and triturated in glial medium (Table 1).

Cells were then plated on 12 mm coverslips coated with 0.1 mg/ml poly-D-lysine and 5 µg/ml laminin and maintained in neuronal media. Every 4 days, half the media was replaced with fresh media. The materials used for the preparation and maintenance of midbrain neuronal culture are outlined in Table 1.

Positive and negative control cell lines: All cell cultures were maintained at 37^{o}C with 5% CO_2 and all cell culture supplies are listed in Table 2. HEK293 cells[45] are not thought to express TH and so were used as a negative expression control and were cultured as described previously[46,47]. PC12 cells express TH[48] and were used as a positive control. The cells were cultured as described by Cartier et al. 2010[49]. CHO cells were cultured as previously described[50], and were used as a negative control for TH expression.

PBMC isolation

PBMCs express TH[43,51]. As previously published[51], whole blood was collected in K2EDTA vacutainer blood collection tubes (BD, 366643) and held at room temperature for up to 2 hours prior to PBMC isolation. Briefly, blood from healthy volunteers and PD patients was overlaid in Leucosep tubes (Table 2) for PBMC isolation, centrifuged for 20 minutes at 400g with brakes turned off and acceleration set to minimum. PBMCs were collected from the interphase of Ficoll and PBS, transferred to a fresh 15mL conical tube, resuspended in 8mL sterile PBS and centrifuged for 10 minutes at 100g, and repeated twice more. Cells were counted with a hemacytometer using trypan blue exclusion of dead cells, and density-adjusted for downstream applications.

Magnetic monocyte isolation

PBMCs are composed of multiple cell subsets[52], each with distinct function and catecholamine sensitivity[53,54] – for example, lymphocyte regulation by catecholamines dopamine and NOR[5,6,55] have been studied for several decades[8,18,56,57], while data regarding catecholamine function in myeloid lineage cells including monocytes is less abundant. In this study, we were narrowly focused on studying peripheral monocytes which we and others have

previously shown to express TH[9,51,58-60]. Because PBMCs comprise a variety of immune cell types, we used immunomagnetic enrichment to obtain a greater than 95% CD14+ monocytes that were utilized in assays described in the current study. Supplementary Figure 2 shows representative flow cytometry data from routine verification of monocyte enrichment. (Supplementary Figure 2).

CD14+ monocytes express TH[51]. Primary CD14+ monocytes were isolated using Biolegend MojoSort magnetic isolation kit (Biolegend, 480094) per manufacturer's instructions. Briefly, 20 million total PBMCs were counted, density adjusted to 1 million cells/uL, resuspended in MojoSort buffer, and incubated with TruStain Fc-block for 10 minutes at room temperature, followed by 1:10 anti-CD14 magnetic nanobeads for 15 minutes on ice. Following 2 washes with 2.5mL ice-cold MojoSort buffer, cell pellet was resuspended in 2.5mL MojoSort buffer and subject to three rounds of magnetic isolation per manufacturer's instructions. The resulting cell pellet was washed to remove remaining non-CD14+ cells and subject to cell lysis as detailed below.

Preparation of cell lysates

Adherent cells in culture were lifted using 0.02% EDTA in PBS, diluted with 5 volumes of PBS, and centrifuged at 100 x *g*. Non-adherent cells (PC12) were centrifuged at 100 x *g* for 5 minutes at room temperature, and cell pellets were washed 3 times with 5 volumes of sterile PBS. Primary macrophages and primary murine neuron cultures were washed thrice with ice-cold PBS, on ice. Cell pellets and adherent primary cells were then lysed in ice-cold lysis buffer (10mM NaCl, 10% glycerol (v/v), 1mM EDTA, 1mM EGTA, and HEPES 20mM, pH 7.6), with Triton X-100 added to a final concentration of 1%, containing 1x protease inhibitor cocktail (Millipore-Sigma, 539131) for one hour at 4^{o}C with rotation. Resulting lysate was centrifuged at 12,000 x *g* for 15 minutes at 4^{o}C. Supernatant was set aside for protein quantification by Lowry assay (Biorad, 5000112) and the remainder was stored at -80^{o}C until use for downstream assays.

Western blot

Reagents, antibodies and equipment are outlined in Tables 2, 3 and 4. Samples of PC12 lysate (5ug) and recombinant TH protein (120ng, 60ng, 30ng, 15ng, 7.5ng, 3.75ng, and 1.875ng) were incubated in Laemmli sample buffer containing 10% beta-mercaptoethanol at 37ºC for 30 minutes, separated by SDS-PAGE on 10% bis/polyacrylamide gels, and transferred to nitrocellulose membranes. After first blocking for 1 hour in TBS-T (50mM Tris-HCl, 150mM NaCl, and 0.1% Tween 20) containing 5% dry milk (blocking buffer), then incubated with primary antibody against TH (Table 4) overnight at 4ºC. Membranes were then incubated with an appropriate secondary antibody (Table 4) for 1 hour at room temperature with agitation. Following all antibody steps, membranes were washed three times for 5 minutes each using TBS-T. TH was visualized using the Licor Odyssey (Table 2). Absorption controls were performed as followed: the primary antibodies were pre-incubated with 20ug/mL recombinant TH protein for 30 minutes on ice, then were used to confirm primary antibody specificity (Table 3, Figure 2C-D).

Immunohistochemistry

Human tissues were sectioned at 40µm on a vibrating microtome and subjected to antigen retrieval in citrate buffer (10mM citric acid, 2mM EDTA, 2% Tween-20, pH 6.2) at 96ºC for 30 minutes, and then allowed to cool to room temperature. PFA-perfused mouse brain tissues were also sectioned at 40 µm on a vibrating microtome.

Human and murine brain tissues were quenched for 20 minutes with 3% hydrogen peroxide, blocked and permeabilized at 37ºC for 1 hour in PBS containing 5% normal goat serum and 0.5% TritonX-100. Primary antibodies RPCA-TH and MCA-4H2 (1:500 and 1:100 dilution, respectively, Table 4) were incubated overnight, followed by secondaries conjugated to HRP (1:250, Table 4), incubated for 1 hour at room temperature. Isotype control antibodies (Biolegend, Table 1) were used to confirm specificity of RPCA-TH and MCA-4H2. Sections were detected with HRP-substrate NiDAB (Vector Labs, Table 3).

Detection antibody (RPCA-TH) Biotinylation

EZ-Link Sulfo-NHS-LC-Biotin (A39257, Thermo Scientific) at 20-fold molar biotin was used according to the manufacturer's protocol. Anti-biotin antibody was concentrated to 2mg/mL, pH was adjusted to 8.0 at room temperature. The conjugate was purified by gel filtration on a Biorad 10DG column (cat 732-2010) at room temperature.

ELISA for TH

Antibodies used for ELISA are described in Table 1. Ten lanes of an Immulon 4 HBX High-Binding 96 well plate were coated with 100uL per well of 1:1,000 dilution of 1mg/mL mouse anti-TH (MCA-4H2) in coating buffer (28.3mM Na_2CO_3, 71.42mM $NaHCO_3$, pH 9.6) for 20 hours at 4^{o}C. Edge lanes 1 and 12 were left empty. Wells were blocked with 5% fat free milk in 1x TBS (pH 7.4) for 1 hour at room temperature on an orbital shaker set to 90rpm. To produce a standard curve, two standard curve lanes were generated, with six serial dilutions, beginning at 10ng/mL and 1ng/mL in TBS-T containing 1% fat free milk (with the last well in each standard curve lane left with incubation buffer only as a blank. Remaining wells were incubated in duplicate with 100 microliters of lysates from 1.5 million cells of interest. Incubation was completed for 20 hours at 4^{o}C on an ELISA shaker set to 475 rpm.

After each well was washed and aspirated 6 times with TBS-T, affinity purified polyclonal rabbit anti-TH (EnCor, RPCA-TH) conjugated to biotin was diluted 1:6,000 from a stock concentration of 1.65mg/mL in TBS-T with 1% fat-free milk and incubated for 1 hour at room temperature at 425rpm. 100uL Avidin-HRP (Vector labs, A-2004), diluted 1:2,500 in TBS-T with 1% fat-free milk, was added to each well following washing as described above, and incubated for 1 hour at room temperature at 425rpm. Following final washes, 150uL room temperature TMB-ELISA reagent (Thermo Fisher, 34028) was added to each well. The reaction was allowed to continue for 20 minutes, protected from light, and stopped by addition of 50uL 2N H_2SO_4. The plate was immediately read at 450nm. Absorption controls (Figure 4) were conducted by pre-incubating MCA-4H2 and RPCA-TH with a 20-fold excess concentration of recombinant TH

protein for 30 minutes on ice, prior to addition to the ELISA plate, followed by the remainder of the protocol described above.

Duplicate standard and sample wells were averaged, and background-subtracted based on blank wells. The concentration of TH for each experimental group was calculated using a quadratic curve equation calculated in Graphpad Prism 8, then normalized to total protein concentration per sample as calculated using the Lowry assay. Samples which produced negative values for TH concentration were considered below detection threshold, and therefore assigned a value of 0. Final TH values shown are presented as pg TH/mg total protein after multiplication of the nanogram TH value by 1,000 to show TH as picogram TH/milligram total protein.

***In vitro* stimulation/treatment with TNFα, tissue plasminogen activator (TPA), TNFα inhibitor XPro1595 and IL6**

Monocytes were isolated from total PBMCs prepared as described above[51] using negative selection (Biolegend, 480048) per manufacturer's instructions. Total PBMCs were Fc-blocked to reduce nonspecific binding, followed by incubations with biotin-conjugated antibody cocktail containing antibodies against all subsets except CD14 (negative selection), followed by incubation with magnetic-Avidin beads, allowing all subsets other than CD14+ monocytes to be bound to the magnet. Monocyte purity/enrichment was routinely verified to confirm that the final cell population was greater than 95% pure CD14+ cells (Figure S2). CD14+ monocytes were collected from the supernatant fraction, washed, counted and density adjusted such that 2 million CD14+ monocytes were seeded per well (Figure 5A) and treated for 4 hours with vehicle, TPA (100ng/mL, Biolegend, 755802)[7], TNFα (17ng/mL, Biolegend, 570102)[61], XPro1595 (50ng/mL), or IL6 (17ng/mL) in an ultra-low-adherence 6-well plate (Corning, 3471) to prevent adherence. Suspended cells from each treatment group were aspirated and placed in a 15mL conical tube, with any remaining adherent cells detached by incubation with 700uL Accumax

solution for 3 minutes (Innovative Cell Technologies, AM105) and added to suspended cells. After pelleting cells by centrifugation (3 minutes x 100g, room temperature), cells were assayed by either flow cytometry[51] or lysed for ELISA as stated above ("Preparation of cell lysates").

As previously published[51], cells for flow cytometry were fixed and permeabilized (eBioscience, 88-8824-00), and stained for intracellular marker TH (Millipore-Sigma, AB152, 1:100) followed by a species-specific secondary (anti-Rabbit BV421, BD, 565014). After resuspending the sample in a final volume of 250uL PBS, 5uL of Invitrogen CountBright Absolute Counting Beads (5000 beads/mL, Invitrogen, C36950) were added just prior to data acquisition (Sony Spectral Analyzer, SP6800). Monocytes were gated for single cells and positive TH expression (Figure 5B), and normalized to counting beads in each sample to obtain an absolute count of TH+ monocytes per uL suspension.

Statistics

A two-tailed, unpaired T test was used to compare TH quantity in PD patients versus healthy control. In this experiment, $P<0.05$ was considered statistically significant. One-way ANOVA with Tukey's correction for multiple comparisons was used to compare TH-expressing monocytes assayed by flow cytometry and ELISA following treatment with TPA, TNFα, XPro1595, IL6 or Vehicle. $P<0.05$ was considered statistically significant.

Data Availability

All data will be made available upon reasonable request.

Acknowledgements: This work was funded by T32-NS082128 (to A.G.), National Center for Advancing Translational Sciences of the National Institutes of Health under University of Florida Clinical and Translational Science Awards TL1TR001428 and UL1TR001427 (to A.G.), R01NS071122-07A1 (to H. K.), NIDA Grant R01DA026947-10, National Institutes of Health Office of the Director Grant 1S10OD020026-01 (to H. K.), UF-Fixel Institute Developmental Fund, DA043895 (to H.K.), by the University of Florida McKnight Brain Institute (MBI) (to A.G.), by the Bryan Robinson Foundation (to A.G.) and by The Karen Toffler Charitable Trust (to A.G.).

Author Contributions

M.F., M.B., G.S., A.C., D.R.M., C.A.H., A.D, and A.G., performed experiments, contributed written portions, figures and methods to this manuscript. P.M., M.G.T., I.M., A.R.Z., M.S.O., W.J.S., H.K., and A.G., supervised, designed experiments in addition to direct contributions to the manuscript.

Competing Interests

The authors declare that they have no financial or non-financial conflicts of interest with the contents of this article. The content is solely the responsibility of the authors and does not necessarily represent the official views of the National Institutes of Health.

References

1 Molinoff, P. B. & Axelrod, J. Biochemistry of catecholamines. *Annu Rev Biochem* **40**, 465-500, doi:10.1146/annurev.bi.40.070171.002341 (1971).

2 Nagatsu, T., Levitt, M. & Udenfriend, S. TYROSINE HYDROXYLASE. THE INITIAL STEP IN NOREPINEPHRINE BIOSYNTHESIS. *J Biol Chem* **239**, 2910-2917 (1964).

3 Berod, A., Biguet, N. F., Dumas, S., Bloch, B. & Mallet, J. Modulation of tyrosine hydroxylase gene expression in the central nervous system visualized by in situ hybridization. *Proc Natl Acad Sci U S A* **84**, 1699-1703, doi:10.1073/pnas.84.6.1699 (1987).

4 Bertler, A. & Rosengren, E. Occurrence and distribution of catechol amines in brain. *Acta Physiol Scand* **47**, 350-361 (1959).

5 Marino, F. *et al.* Endogenous catecholamine synthesis, metabolism storage, and uptake in human peripheral blood mononuclear cells. *Exp Hematol* **27**, 489-495 (1999).

6 Cosentino, M. *et al.* Endogenous catecholamine synthesis, metabolism, storage and uptake in human neutrophils. *Life Sci* **64**, 975-981, doi:10.1016/s0024-3205(99)00023-5 (1999).

7 Cosentino, M. *et al.* Catecholamine production and tyrosine hydroxylase expression in peripheral blood mononuclear cells from multiple sclerosis patients: effect of cell stimulation and possible relevance for activation-induced apoptosis. *J Neuroimmunol* **133**, 233-240, doi:10.1016/s0165-5728(02)00372-7 (2002).

8 Cosentino, M. *et al.* Interferon-gamma and interferon-beta affect endogenous catecholamines in human peripheral blood mononuclear cells: implications for multiple sclerosis. *J Neuroimmunol* **162**, 112-121, doi:10.1016/j.jneuroim.2005.01.019 (2005).

9 Matt, S. M. & Gaskill, P. J. Where Is Dopamine and how do Immune Cells See it?: Dopamine-Mediated Immune Cell Function in Health and Disease. *J Neuroimmune Pharmacol*, doi:10.1007/s11481-019-09851-4 (2019).

10 Weihe, E., Depboylu, C., Schütz, B., Schäfer, M. K. & Eiden, L. E. Three types of tyrosine hydroxylase-positive CNS neurons distinguished by dopa decarboxylase and VMAT2 co-expression. *Cell Mol Neurobiol* **26**, 659-678, doi:10.1007/s10571-006-9053-9 (2006).

11 Harris, R. C. & Zhang, M. Z. Dopamine, the kidney, and hypertension. *Curr Hypertens Rep* **14**, 138-143, doi:10.1007/s11906-012-0253-z (2012).

12 Wolfovitz, E. *et al.* Derivation of urinary dopamine from plasma dihydroxyphenylalanine in humans. *Clin Sci (Lond)* **84**, 549-557, doi:10.1042/cs0840549 (1993).

13 Mohanty, P. K. *et al.* Myocardial norepinephrine, epinephrine and dopamine concentrations after cardiac autotransplantation in dogs. *J Am Coll Cardiol* **7**, 419-424, doi:10.1016/s0735-1097(86)80515-0 (1986).

14 Fhaner, M. J., Galligan, J. J. & Swain, G. M. Increased catecholamine secretion from single adrenal chromaffin cells in DOCA-salt hypertension is associated with potassium channel dysfunction. *ACS Chem Neurosci* **4**, 1404-1413, doi:10.1021/cn400115v (2013).

15 Leszczyszyn, D. J. *et al.* Secretion of catecholamines from individual adrenal medullary chromaffin cells. *J Neurochem* **56**, 1855-1863, doi:10.1111/j.1471-4159.1991.tb03441.x (1991).

16 Wightman, R. M. *et al.* Temporally resolved catecholamine spikes correspond to single vesicle release from individual chromaffin cells. *Proc Natl Acad Sci U S A* **88**, 10754-10758, doi:10.1073/pnas.88.23.10754 (1991).

17 Gaskill, P. J., Carvallo, L., Eugenin, E. A. & Berman, J. W. Characterization and function of the human macrophage dopaminergic system: implications for CNS disease and drug abuse. *J Neuroinflammation* **9**, 203, doi:10.1186/1742-2094-9-203 (2012).

18 Cosentino, M. *et al.* Human CD4+CD25+ regulatory T cells selectively express tyrosine hydroxylase and contain endogenous catecholamines subserving an autocrine/paracrine inhibitory functional loop. *Blood* **109**, 632-642, doi:10.1182/blood-2006-01-028423 (2007).
19 Lindgren, N. *et al.* Regulation of tyrosine hydroxylase activity and phosphorylation at Ser(19) and Ser(40) via activation of glutamate NMDA receptors in rat striatum. *J Neurochem* **74**, 2470-2477, doi:10.1046/j.1471-4159.2000.0742470.x (2000).
20 Kawahata, I. & Fukunaga, K. Degradation of Tyrosine Hydroxylase by the Ubiquitin-Proteasome System in the Pathogenesis of Parkinson's Disease and Dopa-Responsive Dystonia. *Int J Mol Sci* **21**, doi:10.3390/ijms21113779 (2020).
21 Congo Carbajosa, N. A. *et al.* Tyrosine hydroxylase is short-term regulated by the ubiquitin-proteasome system in PC12 cells and hypothalamic and brainstem neurons from spontaneously hypertensive rats: possible implications in hypertension. *PLoS One* **10**, e0116597, doi:10.1371/journal.pone.0116597 (2015).
22 Johnson, M. E., Salvatore, M. F., Maiolo, S. A. & Bobrovskaya, L. Tyrosine hydroxylase as a sentinel for central and peripheral tissue responses in Parkinson's progression: Evidence from clinical studies and neurotoxin models. *Prog Neurobiol* **165-167**, 1-25, doi:10.1016/j.pneurobio.2018.01.002 (2018).
23 Salvatore, M. F., Calipari, E. S. & Jones, S. R. Regulation of Tyrosine Hydroxylase Expression and Phosphorylation in Dopamine Transporter-Deficient Mice. *ACS Chem Neurosci* **7**, 941-951, doi:10.1021/acschemneuro.6b00064 (2016).
24 Wang, Y., Sung, C. C. & Chung, K. K. K. Novel enhancement mechanism of tyrosine hydroxylase enzymatic activity by nitric oxide through S-nitrosylation. *Scientific Reports* **7**, 44154, doi:10.1038/srep44154 (2017).
25 Daubner, S. C., Le, T. & Wang, S. Tyrosine hydroxylase and regulation of dopamine synthesis. *Arch Biochem Biophys* **508**, 1-12, doi:10.1016/j.abb.2010.12.017 (2011).
26 Blanchard-Fillion, B. *et al.* Nitration and inactivation of tyrosine hydroxylase by peroxynitrite. *J Biol Chem* **276**, 46017-46023, doi:10.1074/jbc.M105564200 (2001).
27 Mogi, M. *et al.* Tumor necrosis factor-alpha (TNF-alpha) increases both in the brain and in the cerebrospinal fluid from parkinsonian patients. *Neurosci Lett* **165**, 208-210, doi:10.1016/0304-3940(94)90746-3 (1994).
28 Hirsch, E. C. *et al.* The role of glial reaction and inflammation in Parkinson's disease. *Ann N Y Acad Sci* **991**, 214-228, doi:10.1111/j.1749-6632.2003.tb07478.x (2003).
29 Harris, J. P. *et al.* Emerging regenerative medicine and tissue engineering strategies for Parkinson's disease. *NPJ Parkinsons Dis* **6**, 4, doi:10.1038/s41531-019-0105-5 (2020).
30 Foffani, G. & Obeso, J. A. A Cortical Pathogenic Theory of Parkinson's Disease. *Neuron* **99**, 1116-1128, doi:10.1016/j.neuron.2018.07.028 (2018).
31 Ichinose, H. *et al.* Quantification of mRNA of tyrosine hydroxylase and aromatic L-amino acid decarboxylase in the substantia nigra in Parkinson's disease and schizophrenia. *J Neural Transm Park Dis Dement Sect* **8**, 149-158, doi:10.1007/bf02250926 (1994).
32 Cosentino, M. *et al.* Stimulation with phytohaemagglutinin induces the synthesis of catecholamines in human peripheral blood mononuclear cells: role of protein kinase C and contribution of intracellular calcium. *J Neuroimmunol* **125**, 125-133, doi:10.1016/s0165-5728(02)00019-x (2002).
33 Mogi, M. *et al.* Homospecific activity (activity per enzyme protein) of tyrosine hydroxylase increases in parkinsonian brain. *J Neural Transm* **72**, 77-82, doi:10.1007/bf01244634 (1988).
34 Kouchaki, E. *et al.* Increased serum levels of TNF-alpha and decreased serum levels of IL-27 in patients with Parkinson disease and their correlation with disease severity. *Clin Neurol Neurosurg* **166**, 76-79, doi:10.1016/j.clineuro.2018.01.022 (2018).

35 Rathnayake, D., Chang, T. & Udagama, P. Selected serum cytokines and nitric oxide as potential multi-marker biosignature panels for Parkinson disease of varying durations: a case-control study. *BMC Neurol* **19**, 56, doi:10.1186/s12883-019-1286-6 (2019).
36 Qin, X. Y., Zhang, S. P., Cao, C., Loh, Y. P. & Cheng, Y. Aberrations in Peripheral Inflammatory Cytokine Levels in Parkinson Disease: A Systematic Review and Meta-analysis. *JAMA Neurol* **73**, 1316-1324, doi:10.1001/jamaneurol.2016.2742 (2016).
37 McCoy, M. K. & Tansey, M. G. TNF signaling inhibition in the CNS: implications for normal brain function and neurodegenerative disease. *J Neuroinflammation* **5**, 45, doi:10.1186/1742-2094-5-45 (2008).
38 McCoy, M. K. *et al.* Blocking soluble tumor necrosis factor signaling with dominant-negative tumor necrosis factor inhibitor attenuates loss of dopaminergic neurons in models of Parkinson's disease. *J Neurosci* **26**, 9365-9375, doi:10.1523/JNEUROSCI.1504-06.2006 (2006).
39 Lee, J. K., Tran, T. & Tansey, M. G. Neuroinflammation in Parkinson's disease. *J Neuroimmune Pharmacol* **4**, 419-429, doi:10.1007/s11481-009-9176-0 (2009).
40 Su, X. *et al.* Synuclein activates microglia in a model of Parkinson's disease. *Neurobiol Aging* **29**, 1690-1701, doi:10.1016/j.neurobiolaging.2007.04.006 (2008).
41 Block, M. L. & Hong, J. S. Microglia and inflammation-mediated neurodegeneration: multiple triggers with a common mechanism. *Prog Neurobiol* **76**, 77-98, doi:10.1016/j.pneurobio.2005.06.004 (2005).
42 Kim, Y. S. & Joh, T. H. Microglia, major player in the brain inflammation: their roles in the pathogenesis of Parkinson's disease. *Exp Mol Med* **38**, 333-347, doi:10.1038/emm.2006.40 (2006).
43 Mackie, P. *et al.* The dopamine transporter: An unrecognized nexus for dysfunctional peripheral immunity and signaling in Parkinson's Disease. *Brain Behav Immun* **70**, 21-35, doi:10.1016/j.bbi.2018.03.020 (2018).
44 Braak, H. & Del Tredici, K. Invited Article: Nervous system pathology in sporadic Parkinson disease. *Neurology* **70**, 1916-1925, doi:10.1212/01.wnl.0000312279.49272.9f (2008).
45 Graham, F. L., Smiley, J., Russell, W. C. & Nairn, R. Characteristics of a human cell line transformed by DNA from human adenovirus type 5. *J Gen Virol* **36**, 59-74, doi:10.1099/0022-1317-36-1-59 (1977).
46 Goodwin, J. S. *et al.* Amphetamine and methamphetamine differentially affect dopamine transporters in vitro and in vivo. *J Biol Chem* **284**, 2978-2989, doi:10.1074/jbc.M805298200 (2009).
47 Saha, K. *et al.* Intracellular methamphetamine prevents the dopamine-induced enhancement of neuronal firing. *J Biol Chem* **289**, 22246-22257, doi:10.1074/jbc.M114.563056 (2014).
48 Greene, L. A. & Tischler, A. S. Establishment of a noradrenergic clonal line of rat adrenal pheochromocytoma cells which respond to nerve growth factor. *Proc Natl Acad Sci U S A* **73**, 2424-2428, doi:10.1073/pnas.73.7.2424 (1976).
49 Cartier, E. A. *et al.* A biochemical and functional protein complex involving dopamine synthesis and transport into synaptic vesicles. *J Biol Chem* **285**, 1957-1966, doi:10.1074/jbc.M109.054510 (2010).
50 Swant, J. *et al.* alpha-Synuclein stimulates a dopamine transporter-dependent chloride current and modulates the activity of the transporter. *J Biol Chem* **286**, 43933-43943, doi:10.1074/jbc.M111.241232 (2011).
51 Gopinath, A. *et al.* A novel approach to study markers of dopamine signaling in peripheral immune cells. *J Immunol Methods* **476**, 112686, doi:10.1016/j.jim.2019.112686 (2020).
52 Corkum, C. P. *et al.* Immune cell subsets and their gene expression profiles from human PBMC isolated by Vacutainer Cell Preparation Tube (CPT™) and standard density gradient. *BMC Immunol* **16**, 48, doi:10.1186/s12865-015-0113-0 (2015).

53 Flierl, M. A., Rittirsch, D., Huber-Lang, M., Sarma, J. V. & Ward, P. A. Catecholamines-crafty weapons in the inflammatory arsenal of immune/inflammatory cells or opening pandora's box? *Mol Med* **14**, 195-204, doi:10.2119/2007-00105.Flierl (2008).

54 Flierl, M. A. *et al.* Upregulation of phagocyte-derived catecholamines augments the acute inflammatory response. *PLoS One* **4**, e4414, doi:10.1371/journal.pone.0004414 (2009).

55 Torres, K. C. *et al.* Norepinephrine, dopamine and dexamethasone modulate discrete leukocyte subpopulations and cytokine profiles from human PBMC. *J Neuroimmunol* **166**, 144-157, doi:10.1016/j.jneuroim.2005.06.006 (2005).

56 Kustrimovic, N. *et al.* Dopaminergic Receptors on CD4+ T Naive and Memory Lymphocytes Correlate with Motor Impairment in Patients with Parkinson's Disease. *Sci Rep* **6**, 33738, doi:10.1038/srep33738 (2016).

57 Bergquist, J., Tarkowski, A., Ekman, R. & Ewing, A. Discovery of endogenous catecholamines in lymphocytes and evidence for catecholamine regulation of lymphocyte function via an autocrine loop. *Proc Natl Acad Sci U S A* **91**, 12912-12916, doi:10.1073/pnas.91.26.12912 (1994).

58 Eugenin, E. A., Gaskill, P. J. & Berman, J. W. Tunneling nanotubes (TNT) are induced by HIV-infection of macrophages: a potential mechanism for intercellular HIV trafficking. *Cell Immunol* **254**, 142-148, doi:10.1016/j.cellimm.2008.08.005 (2009).

59 Nolan, R. & Gaskill, P. J. The role of catecholamines in HIV neuropathogenesis. *Brain Res* **1702**, 54-73, doi:10.1016/j.brainres.2018.04.030 (2019).

60 Nolan, R. A., Muir, R., Runner, K., Haddad, E. K. & Gaskill, P. J. Role of Macrophage Dopamine Receptors in Mediating Cytokine Production: Implications for Neuroinflammation in the Context of HIV-Associated Neurocognitive Disorders. *J Neuroimmune Pharmacol* **14**, 134-156, doi:10.1007/s11481-018-9825-2 (2019).

61 Merry, K. & Gowen, M. The transcriptional control of TGF-beta in human osteoblast-like cells is distinct from that of IL-1 beta. *Cytokine* **4**, 171-179, doi:10.1016/1043-4666(92)90052-s (1992).

62 Pickel, V. M., Joh, T. H., Field, P. M., Becker, C. G. & Reis, D. J. Cellular localization of tyrosine hydroxylase by immunohistochemistry. *J Histochem Cytochem* **23**, 1-12, doi:10.1177/23.1.234988 (1975).

63 Kastner, A., Hirsch, E. C., Herrero, M. T., Javoy-Agid, F. & Agid, Y. Immunocytochemical quantification of tyrosine hydroxylase at a cellular level in the mesencephalon of control subjects and patients with Parkinson's and Alzheimer's disease. *J Neurochem* **61**, 1024-1034, doi:10.1111/j.1471-4159.1993.tb03616.x (1993).

64 Yan, H. Q. *et al.* Delayed increase of tyrosine hydroxylase expression in rat nigrostriatal system after traumatic brain injury. *Brain Res* **1134**, 171-179, doi:10.1016/j.brainres.2006.11.087 (2007).

65 Witkovsky, P., Gabriel, R. & Krizaj, D. Anatomical and neurochemical characterization of dopaminergic interplexiform processes in mouse and rat retinas. *J Comp Neurol* **510**, 158-174, doi:10.1002/cne.21784 (2008).

66 Giguere, N. *et al.* Increased vulnerability of nigral dopamine neurons after expansion of their axonal arborization size through D2 dopamine receptor conditional knockout. *PLoS Genet* **15**, e1008352, doi:10.1371/journal.pgen.1008352 (2019).

67 Colon-Perez, L. M. *et al.* Functional connectivity, behavioral and dopaminergic alterations 24 hours following acute exposure to synthetic bath salt drug methylenedioxypyrovalerone. *Neuropharmacology* **137**, 178-193, doi:10.1016/j.neuropharm.2018.04.031 (2018).

68 Contini, M. & Raviola, E. GABAergic synapses made by a retinal dopaminergic neuron. *Proc Natl Acad Sci U S A* **100**, 1358-1363, doi:10.1073/pnas.0337681100 (2003).

69 Feinstein, P., Bozza, T., Rodriguez, I., Vassalli, A. & Mombaerts, P. Axon guidance of mouse olfactory sensory neurons by odorant receptors and the beta2 adrenergic receptor. *Cell* **117**, 833-846, doi:10.1016/j.cell.2004.05.013 (2004).

70 Shaw, G., Morse, S., Ararat, M. & Graham, F. L. Preferential transformation of human neuronal cells by human adenoviruses and the origin of HEK 293 cells. *Faseb j* **16**, 869-871, doi:10.1096/fj.01-0995fje (2002).
71 Miller, D. R. *et al.* Methamphetamine regulation of activity and topology of ventral midbrain networks. *PLoS One* **14**, e0222957, doi:10.1371/journal.pone.0222957 (2019).
72 Trudeau, L. E. *et al.* The multilingual nature of dopamine neurons. *Prog Brain Res* **211**, 141-164, doi:10.1016/b978-0-444-63425-2.00006-4 (2014).
73 Morales, M. & Margolis, E. B. Ventral tegmental area: cellular heterogeneity, connectivity and behaviour. *Nature Reviews Neuroscience* **18**, 73-85, doi:10.1038/nrn.2016.165 (2017).
74 Caggiu, E. *et al.* Inflammation, Infectious Triggers, and Parkinson's Disease. *Front Neurol* **10**, 122, doi:10.3389/fneur.2019.00122 (2019).
75 Kozina, E. *et al.* Mutant LRRK2 mediates peripheral and central immune responses leading to neurodegeneration in vivo. *Brain* **141**, 1753-1769, doi:10.1093/brain/awy077 (2018).
76 Rentzos, M. *et al.* Circulating interleukin-15 and RANTES chemokine in Parkinson's disease. *Acta Neurol Scand* **116**, 374-379, doi:10.1111/j.1600-0404.2007.00894.x (2007).
77 Brodacki, B. *et al.* Serum interleukin (IL-2, IL-10, IL-6, IL-4), TNFalpha, and INFgamma concentrations are elevated in patients with atypical and idiopathic parkinsonism. *Neurosci Lett* **441**, 158-162, doi:10.1016/j.neulet.2008.06.040 (2008).
78 Dufek, M. *et al.* Serum inflammatory biomarkers in Parkinson's disease. *Parkinsonism Relat Disord* **15**, 318-320, doi:10.1016/j.parkreldis.2008.05.014 (2009).
79 Deleidi, M. & Gasser, T. The role of inflammation in sporadic and familial Parkinson's disease. *Cell Mol Life Sci* **70**, 4259-4273, doi:10.1007/s00018-013-1352-y (2013).
80 Jenei-Lanzl, Z. *et al.* Anti-inflammatory effects of cell-based therapy with tyrosine hydroxylase-positive catecholaminergic cells in experimental arthritis. *Ann Rheum Dis* **74**, 444-451, doi:10.1136/annrheumdis-2013-203925 (2015).
81 Miller, L. E., Grifka, J., Schölmerich, J. & Straub, R. H. Norepinephrine from synovial tyrosine hydroxylase positive cells is a strong indicator of synovial inflammation in rheumatoid arthritis. *J Rheumatol* **29**, 427-435 (2002).
82 Doll, D. N., Rellick, S. L., Barr, T. L., Ren, X. & Simpkins, J. W. Rapid mitochondrial dysfunction mediates TNF-alpha-induced neurotoxicity. *J Neurochem* **132**, 443-451, doi:10.1111/jnc.13008 (2015).
83 Giustarini, G. *et al.* Tissue influx of neutrophils and monocytes is delayed during development of trovafloxacin-induced tumor necrosis factor-dependent liver injury in mice. *J Appl Toxicol* **38**, 753-765, doi:10.1002/jat.3585 (2018).
84 Nakai, Y., Hamagaki, S., Takagi, R., Taniguchi, A. & Kurimoto, F. Plasma concentrations of tumor necrosis factor-alpha (TNF-alpha) and soluble TNF receptors in patients with anorexia nervosa. *J Clin Endocrinol Metab* **84**, 1226-1228, doi:10.1210/jcem.84.4.5589 (1999).
85 Turner, D. A. *et al.* Physiological levels of TNFalpha stimulation induce stochastic dynamics of NF-kappaB responses in single living cells. *J Cell Sci* **123**, 2834-2843, doi:10.1242/jcs.069641 (2010).
86 Damas, P. *et al.* Tumor necrosis factor and interleukin-1 serum levels during severe sepsis in humans. *Crit Care Med* **17**, 975-978, doi:10.1097/00003246-198910000-00001 (1989).
87 Kim, K. H. & Sederstrom, J. M. Assaying Cell Cycle Status Using Flow Cytometry. *Curr Protoc Mol Biol* **111**, 28.26.21-28.26.11, doi:10.1002/0471142727.mb2806s111 (2015).
88 Pereira, J. R. *et al.* IL-6 serum levels are elevated in Parkinson's disease patients with fatigue compared to patients without fatigue. *J Neurol Sci* **370**, 153-156, doi:10.1016/j.jns.2016.09.030 (2016).

89 Seppi, K. *et al.* Update on treatments for nonmotor symptoms of Parkinson's disease-an evidence-based medicine review. *Mov Disord* **34**, 180-198, doi:10.1002/mds.27602 (2019).
90 Lindqvist, D. *et al.* Non-motor symptoms in patients with Parkinson's disease - correlations with inflammatory cytokines in serum. *PLoS One* **7**, e47387, doi:10.1371/journal.pone.0047387 (2012).
91 Joers, V. *et al.* Microglia, inflammation and gut microbiota responses in a progressive monkey model of Parkinson's disease: A case series. *Neurobiol Dis* **144**, 105027, doi:10.1016/j.nbd.2020.105027 (2020).
92 O'Reilly, M. L. *et al.* Pharmacological Inhibition of Soluble Tumor Necrosis Factor-Alpha Two Weeks after High Thoracic Spinal Cord Injury Does Not Affect Sympathetic Hyperreflexia. *J Neurotrauma*, doi:10.1089/neu.2020.7504 (2021).

Figure 1. Establishing a reproducible quantitative Bio-ELISA to detect Tyrosine Hydroxylase. A-D) TH is detectable in recombinant form and in PC12 crude lysate using affinity purified rabbit polyclonal TH antibody AB152 (Sigma), and antibodies selected for this ELISA, mouse monoclonal MCA-4H2 (EnCor) and rabbit polyclonal RPCA-TH (EnCor). E) Using AB152, we probed the lower threshold for TH detection *via* serial dilution of purified recombinant TH from 6ug/mL to 0.094ug/mL followed by Western blot and near-Infrared detection, considered to be a sensitive method for protein detection on Western blot. We demonstrate IR detection is reliable to a lower threshold of ~15ng TH. Below this limit, TH detection becomes unreliable with IR detection. F-H) In a series of stepwise experiments designed to increase ELISA sensitivity and decrease background, we achieved lower detection limits of 15pg/mL TH (H). Capture antibody and detection antibody in all three methods were MCA-4H2 (1:1,000 dilution from 1mg/mL) and RPCA-TH (1:6,000 dilution from 1mg/mL). Schematic representation of each method shown on the left with representative standard curve on the right. F) Incubation with detection antibody followed by an HRP-conjugate secondary yielded a lower detection threshold of 125pg/mL. G) Addition of a tertiary layer using anti-rabbit biotin followed by Avidin-HRP improved lower detection threshold to 62.5pg/mL but resulted in increased background. H) Use of biotinylated detection antibody (RPCA-TH-biotin, 1:6,000 dilution from 1.65mg/mL) followed by avidin-HRP yielded the lowest detection threshold of 15 pg/mL, with maximum sensitivity and minimal background. F-H) Insets (red outline) shows magnified lower standard curve to illustrate sensitivity.

Figure 2. Antibodies MCA-4H2 and RPCA-TH reliably detect both native and denatured TH in mouse and human tissue. Human and murine brain sections (40um) were permeabilized, blocked and stained with primary antibodies (MCA-4H2 and RPCA-TH) followed by HRP-conjugated secondaries and detected using diaminobenzidine enhanced with nickel (NiDAB, grey-black). A) MCA-4H2 stains neuromelanin-expressing (brown) TH positive midbrain neurons and neuronal processes (grey-black) with no non-specific staining (secondary only, top

838 panel; isotype control, second panel) in both human and murine tissues. B) RPCA-TH shows
839 similar highly specific staining of midbrain TH positive neurons, confirming antibody specificity.
840 A & B) Human midbrain tissues shown as secondary-only and isotype controls exhibit
841 endogenous neuromelanin (brown), not to be confused with immunostaining. C) Western blot
842 analyses of murine and human striatal tissues reveal similarly specific detection of TH (~63kDa
843 band) in both mouse and human, with minimal non-specific staining in negative control
844 homogenate (parental CHO cell homogenate). (Left – MCA-4H2, right – RPCA-TH). D) Blocking
845 peptide/absorption control followed by western blot detection with either RPCA-TH and MCA-
846 4H2 confirms specificity of both antibodies for TH protein. HSP60 (loading control) is shown
847 below and applies to C-D.
848 **Figure 3. Bio-ELISA reliably quantifies TH in PC12 cells, human macrophages and**
849 **cultured murine dopamine neurons.** A) Using the Bio-ELISA shown in Figure 1G, we
850 quantified TH in four relevant tissues and cultured cells: PC12 (positive control), HEK293
851 (negative control), cultured human macrophages and cultured primary murine dopamine
852 neurons. PC12 cells express very high levels of TH (<10ng TH / mg total protein) relative to
853 human macrophages (~300 pg TH / mg total protein) and primary murine dopamine neurons
854 (~700 pg TH / mg total protein). B) TH values are plotted on a representative standard curve for
855 visual comparison, with inset magnifying the lower end of the standard curve. C) Calculations
856 are shown by which raw TH concentration in ng/mL is normalized to total protein per sample.
857 Samples included in A, each an independent biological replicate, are shown in C. Data are
858 shown as ±SEM.
859 **Figure 4. Absorption controls demonstrate specificity of TH Bio-ELISA.** A) Schematic
860 layout of experimental conditions to assess absorption controls in contrast to optimized Bio-
861 ELISA conditions using PC12 cell lysate. B) Representative standard curve shown to illustrate
862 PC12 cells' TH concentration using optimized Bio-ELISA (blue arrow), absorbed capture
863 antibody (MCA-4H2 preincubated with 20ug/mL recombinant TH, orange arrow), and absorbed

detection antibody (biotinylated RPCA-TH preincubated with 20ug/mL recombinant TH, green arrow). PC12 TH is undetectable after absorption of either capture or detection antibodies, confirming assay specificity.

Figure 5. TH protein is increased in CD14+ monocytes isolated from PD patients. Total CD14+ monocytes were magnetically isolated from 20 million freshly isolated PBMCs derived from whole blood of 11 PD patients and 11 healthy volunteers, immediately lysed in the presence of protease inhibitor and stored at -80°C. Following protein quantification, whole lysate from each sample was added to duplicate wells and assayed for concentration of TH. A) Monocytes isolated from PD patients express significantly greater quantity of TH compared to equivalent monocytes isolated from healthy control subjects (unpaired two-tailed T-test, alpha=0.05, $p<0.05$) B) Mean TH concentration for monocytes from PD patients plotted on a representative standard curve, with inset magnifying the lower end of the curve. C) Calculations are shown by which raw TH concentration in ng/mL is normalized to total protein per sample. Samples included in A, each an independent biological replicate, are shown in C. Data are shown as $\pm$SEM.

Figure 6. TNFα increases number of TH+ monocytes and amount of TH protein per monocyte. A) Total CD14+ monocytes were isolated using negative magnetic selection from 80 million healthy donor PBMCs. Monocytes were seeded into a 6-well ultra-low-adherence plate at 2 million cells per well, and treated with vehicle (media), TPA (100ng/mL, positive control), TNFα (17ng/mL), in duplicate. B) One duplicate was assayed by flow cytometry to detect TH-expressing monocytes, using counting beads as a reference value to quantify the number of TH+ cells. C) Number of TH+ cells were quantified as shown. D) Representative histogram showing one set of samples assayed for TH expressing monocytes following stimulation. E) Both TPA and TNFα induced significant increases in TH-expressing monocytes relative to vehicle, shown as fold-increase relative to vehicle (n=3 per group, one-way ANOVA, $p<0.01$). F)

No increase in total monocytes per condition, relative to vehicle (n=3 per group, one-way ANOVA, n.s.). G) TH concentration in picograms per milligram total protein shows TNFA treatment results in significantly increased TH protein relative to vehicle and TPA (n=5-6 per group, one-way ANOVA, $p<0.001$). H) Mean TH protein level for monocytes treated with vehicle, TPA and TNFα are plotted on a representative standard curve, with the inset magnifying the lower end of the curve. I) Intracellular flow cytometry for Ki67 does not reveal significant differences between vehicle and TNFα treatment groups, confirming a lack of cell proliferation following TNFα treatment. Data are shown as $\pm$SEM.

Figure 7. Inhibition of TNFα blocks increase in number of TH+ monocytes and amount of TH per monocyte. A-B) Acutely isolated monocytes from three healthy donors were seeded at 2 million cells per well in duplicate ultra-low-adherence plates, and treated with TNFα (17ng/mL), XPro1595 (50ng/mL), IL6 (17ng/mL) or combinations thereof as indicated. C) In samples assayed by flow cytometry, using counting beads as a reference value to quantify the number of TH+ cells, co-incubation with TNFα and XPro1595 significantly reduced the number of TH+ monocytes relative to TNFα treatment alone. Treatment with IL6 or IL6 + XPro1595 resulted in no significant change in the number of TH+ monocytes. Values are represented as fold change relative to vehicle (n=3 per group, one way ANOVA, $*P<0.05$, $**P<0.01$). D) TH concentration (picogram per milligram total protein) significantly increases upon TNFα treatment, and is reduced significantly to baseline levels following co-incubation with TNFα and XPro1595. Neither IL6 nor IL6+XPro1595 significantly increased TH quantity (n=3 per group, one way ANOVA, $*P<0.05$). Data are shown as $\pm$SEM.

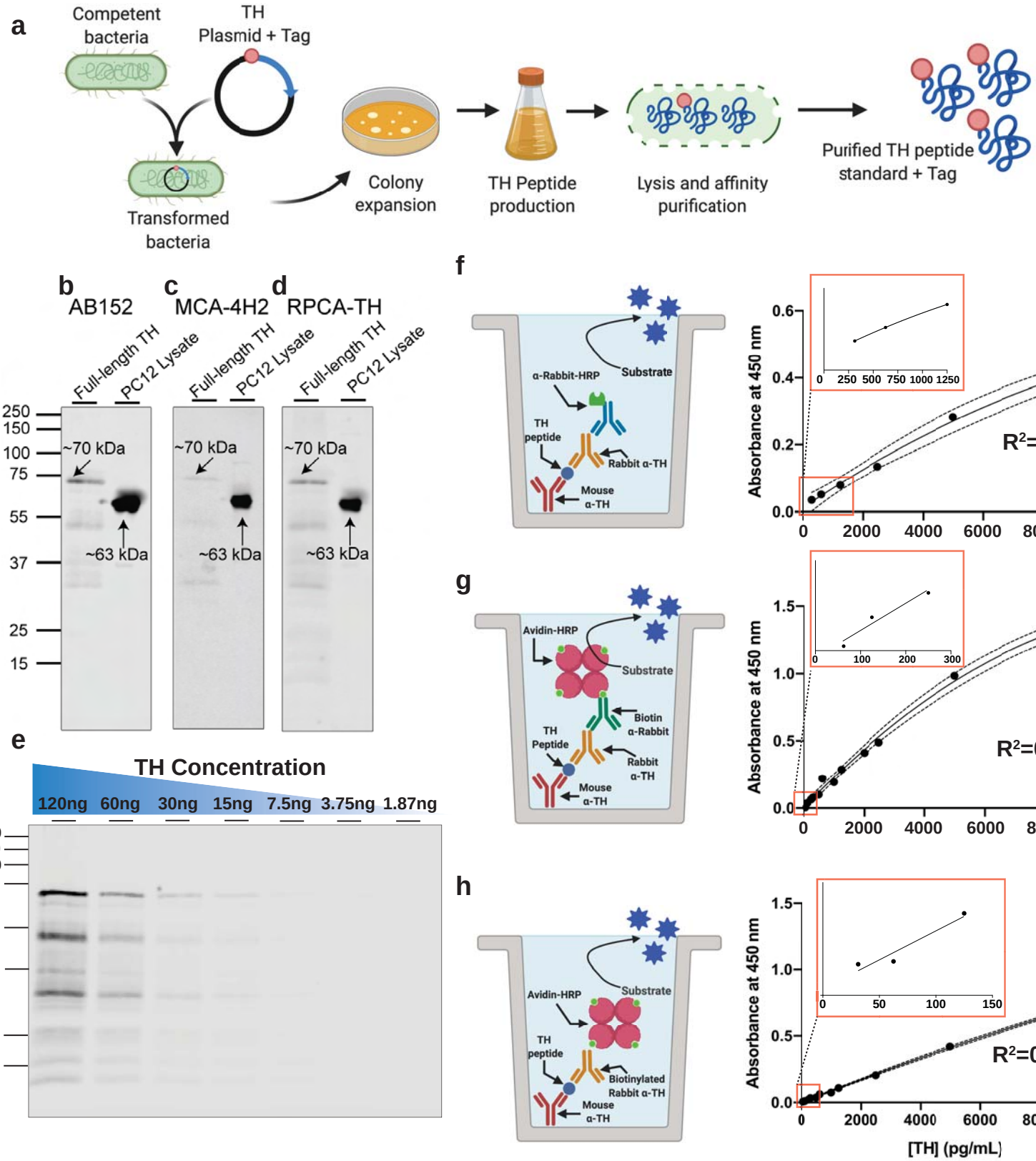
a
Competent bacteria
TH Plasmid + Tag
Transformed bacteria
Colony expansion
TH Peptide production
Lysis and affinity purification
Purified TH peptide standard + Tag
b
AB152
c
MCA-4H2
d
RPCA-TH
Full-length TH
PC12 Lysate
250
150
100
75
55
37
25
15
~70 kDa
~63 kDa
e
TH Concentration
120ng
60ng
30ng
15ng
7.5ng
3.75ng
1.87ng
250
150
100
75
50
37
20
15
f
α-Rabbit-HRP
Substrate
TH peptide
Rabbit α-TH
Mouse α-TH
Absorbance at 450 nm
R²=0.9959
g
Avidin-HRP
Substrate
Biotin α-Rabbit
TH Peptide
Rabbit α-TH
Mouse α-TH
R²=0.9945
h
Avidin-HRP
Substrate
TH peptide
Biotinylated Rabbit α-TH
Mouse α-TH
R²=0.9992
[TH] (pg/mL)

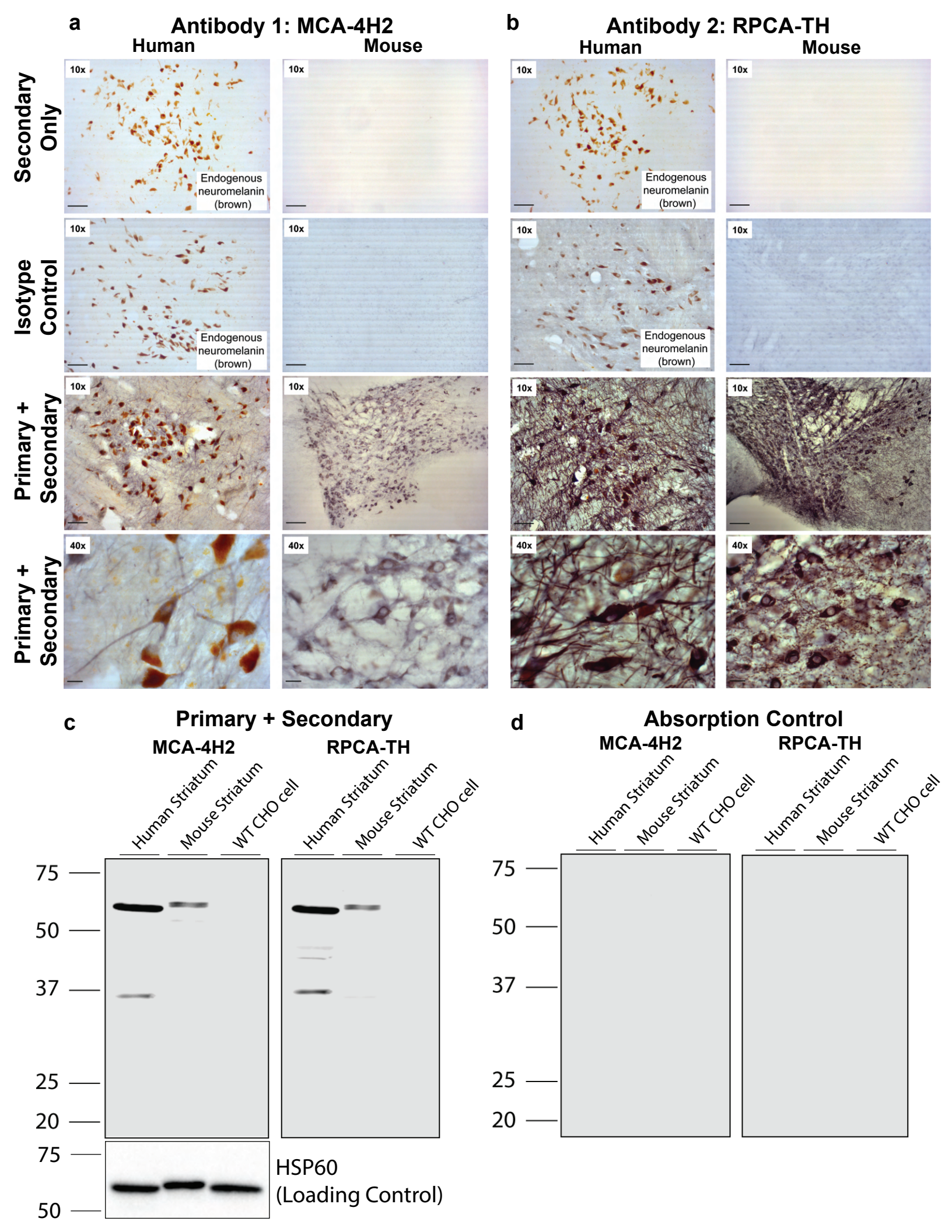
a
Antibody 1: MCA-4H2
Human
Mouse
b
Antibody 2: RPCA-TH
Human
Mouse
Secondary Only
Isotype Control
Primary + Secondary
Primary + Secondary
10x
40x
Endogenous neuromelanin (brown)
c
Primary + Secondary
MCA-4H2
RPCA-TH
Human Striatum
Mouse Striatum
WT CHO cell
75
50
37
25
20
HSP60
(Loading Control)
d
Absorption Control
MCA-4H2
RPCA-TH
Human Striatum
Mouse Striatum
WT CHO cell
75
50
37
25
20

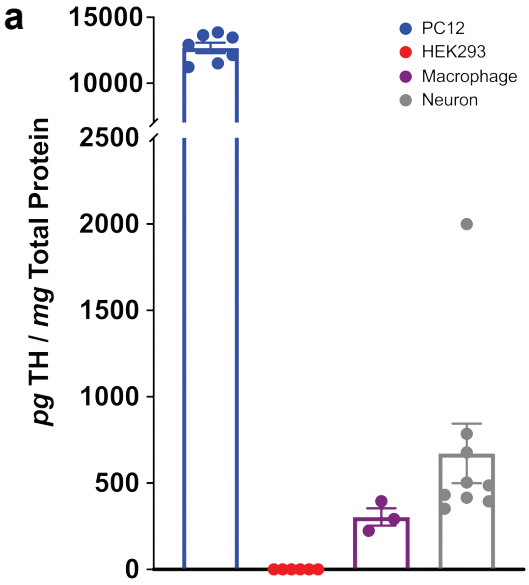

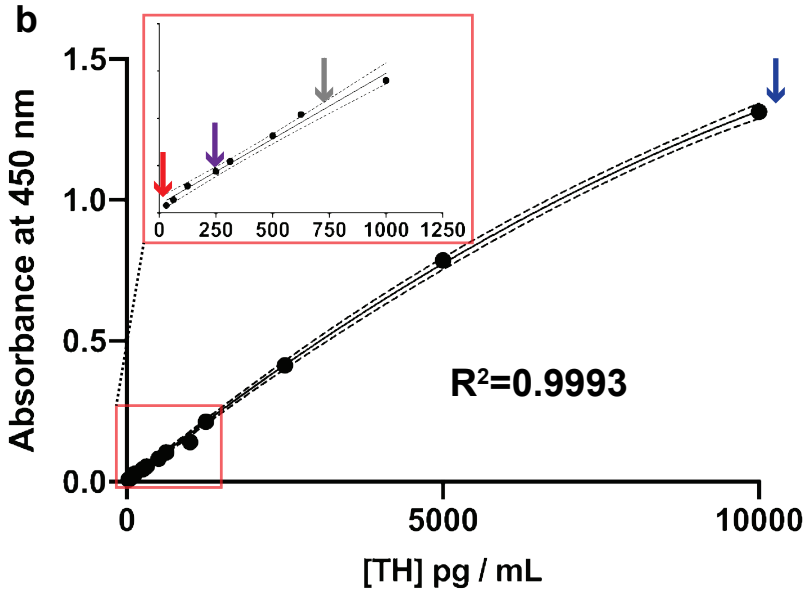

c

TH Concentration Calculations in pg TH per mg Total Protein			
Sample ID	[TH] ng/mL	[Protein] mg/mL	pg TH / mg Protein
PC12	24.552	1.800	13639.816
PC12	15.365	1.190	12911.395
PC12	24.158	2.100	11503.757
PC12	20.208	1.800	11226.728
PC12	24.232	1.800	13462.029
PC12	21.850	1.800	12138.909
PC12	24.870	1.800	13816.439
HEK293	N/D	2.900	N/D
HEK293	N/D	1.000	N/D
HEK293	N/D	1.000	N/D
HEK293	N/D	1.000	N/D
HEK293	N/D	1.000	N/D
HEK293	N/D	1.000	N/D
Macrophage	0.130	0.446	292.087
Macrophage	0.144	0.646	223.685
Macrophage	0.759	1.920	395.295
Neuron	0.568	1.439	394.782
Neuron	0.397	0.920	431.783
Neuron	0.321	0.913	351.731
Neuron	0.259	0.624	415.677
Neuron	0.375	0.772	486.432
Neuron	0.303	0.601	503.478
Neuron	0.542	0.801	676.852
Neuron	0.234	0.298	785.289
Neuron	1.897	0.949	1999.383

a

Absorbtion Control ELISA: Plate Map

	1	2	3	4	5	6	7	8	9	10	11	12
A		Standard Curve				Bio- ELISA	TH protein absorbed MCA-4H2	(Empty)				
B												
C												
D												
E												
F												
G		Blanks					TH protein absorbed Biotin-RPCA-TH					
H		(Empty)										

b

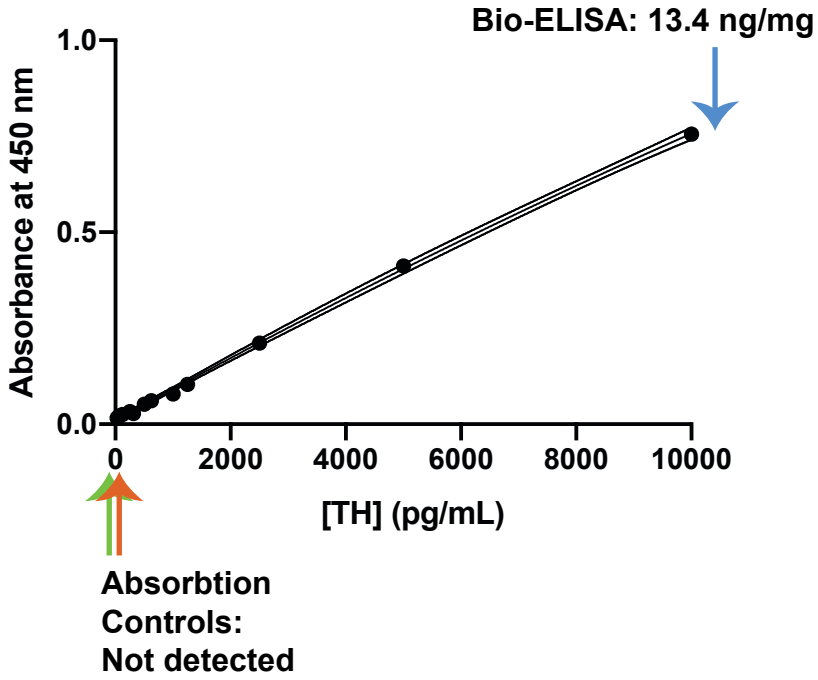

a

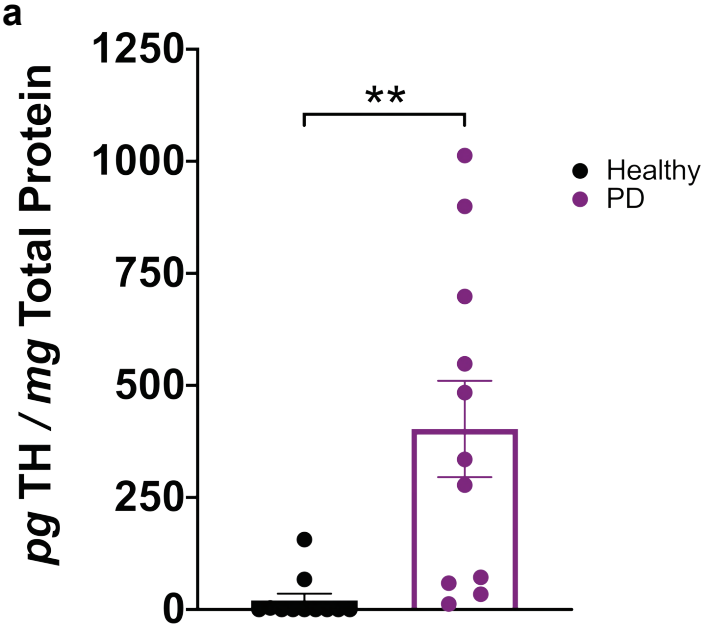

b

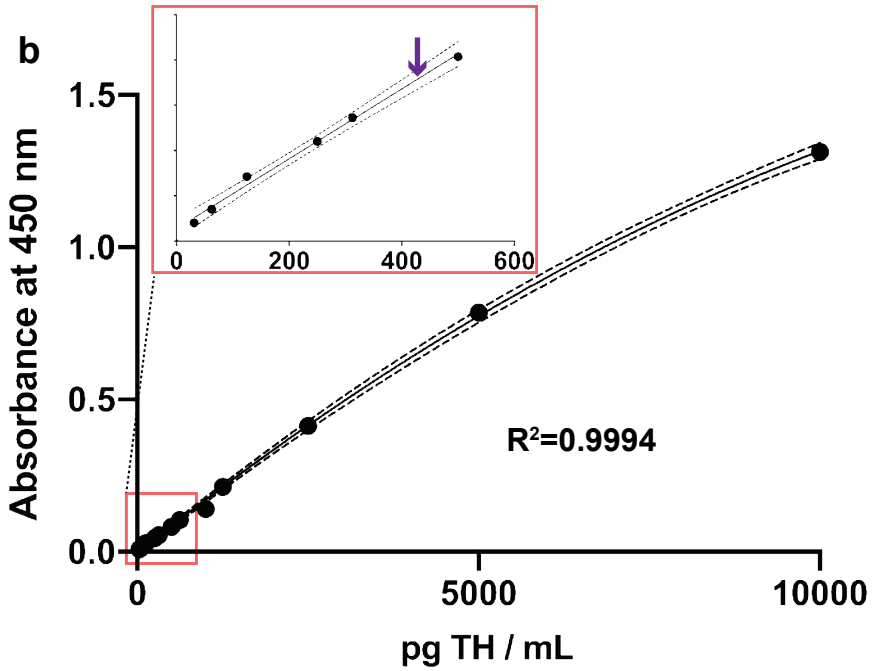

c

TH concentration in CD14+ monocytes of Parkinson's disease patients relative to healthy controls			
Patient ID	**[TH] ng/mL**	**[Protein] mg/mL**	**pg TH / mg Protein**
Parkinson's 149	0.121	1.689	71.827
Parkinson's 150	0.086	1.460	58.651
Parkinson's 151	0.050	1.460	34.213
Parkinson's 154	0.340	1.225	277.646
Parkinson's 155	0.034	2.728	12.525
Parkinson's 161	1.507	1.676	899.557
Parkinson's 163	1.796	1.773	1012.918
Parkinson's 164	1.137	2.074	548.146
Parkinson's 165	1.713	2.452	698.632
Parkinson's 166	1.013	2.093	484.033
Parkinson's 167	0.643	1.918	334.909
Healthy subject 1	0.099	1.471	67.305
Healthy Subject 2	0.007	2.040	3.590
Healthy Subject 3	N/D	1.209	N/D
Healthy Subject 4	N/D	1.047	N/D
Healthy Subject 5	N/D	1.809	N/D
Healthy Subject 6	N/D	1.671	N/D
Healthy Subject 7	N/D	1.178	N/D
Healthy Subject 8	N/D	2.164	N/D
Healthy Subject 9	0.272	1.744	155.893
Healthy Subject 10	N/D	2.181	N/D
Healthy Subject 11	N/D	2.229	N/D

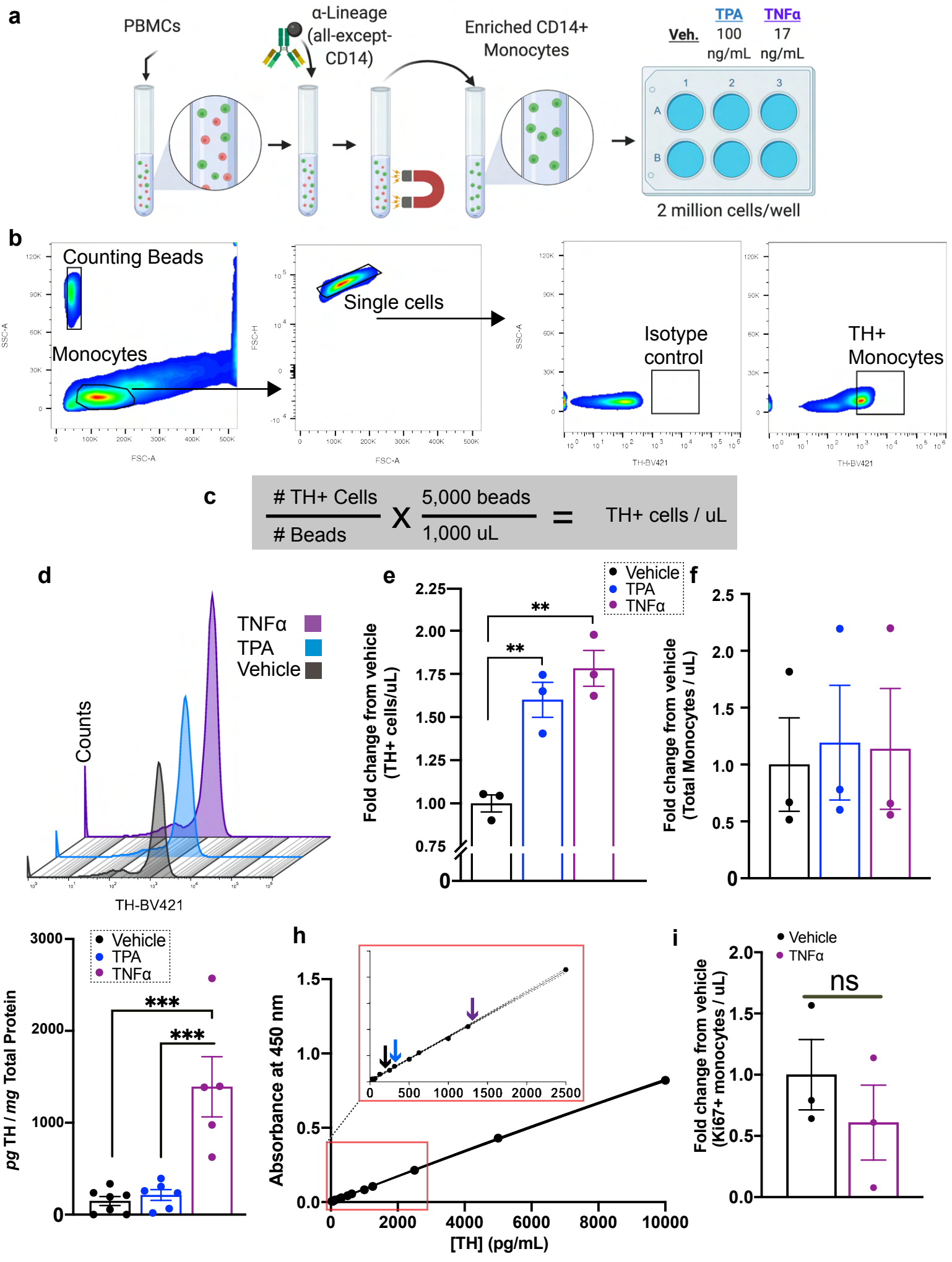
a
PBMCs
α-Lineage (all-except-CD14)
Enriched CD14+ Monocytes
Veh.
TPA 100 ng/mL
TNFα 17 ng/mL
2 million cells/well
b
Counting Beads
Monocytes
Single cells
Isotype control
TH+ Monocytes
SSC-A
FSC-A
FSC-H
TH-BV421
c
TH+ Cells / # Beads X 5,000 beads / 1,000 uL = TH+ cells / uL
d
TNFα
TPA
Vehicle
Counts
TH-BV421
e
Vehicle
TPA
TNFα
Fold change from vehicle (TH+ cells/uL)
f
Fold change from vehicle (Total Monocytes / uL)
g
pg TH / mg Total Protein
h
Absorbance at 450 nm
[TH] (pg/mL)
i
Fold change from vehicle (Ki67+ monocytes / uL)
ns

a

Donor demographics		
Donor ID	**Gender**	**Age**
#1	Male	77
#2	Female	69
#3	Male	50

b

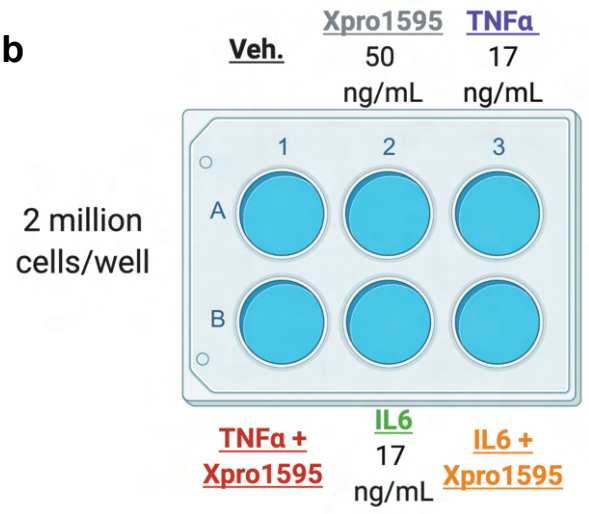

c

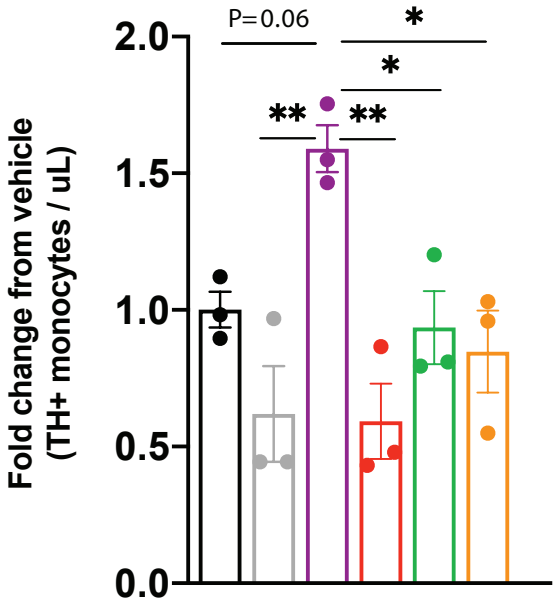

d

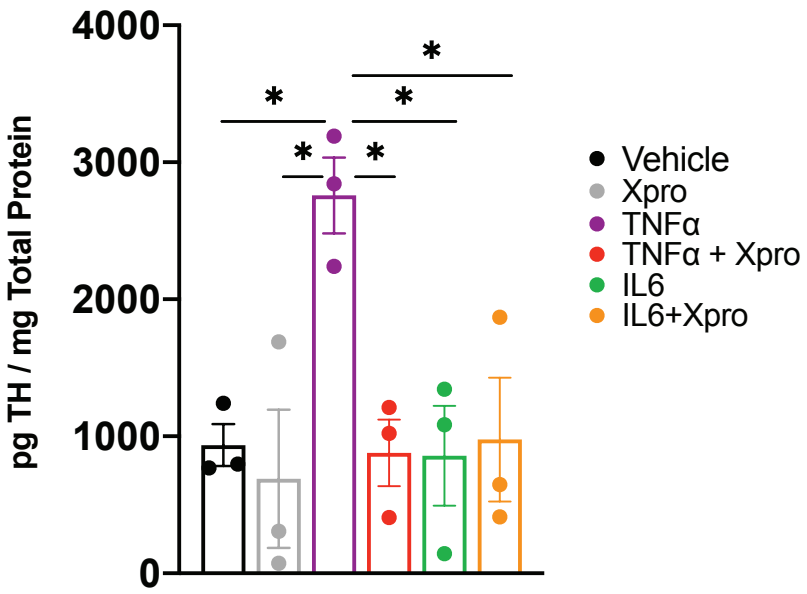

Supplementary Figure 1

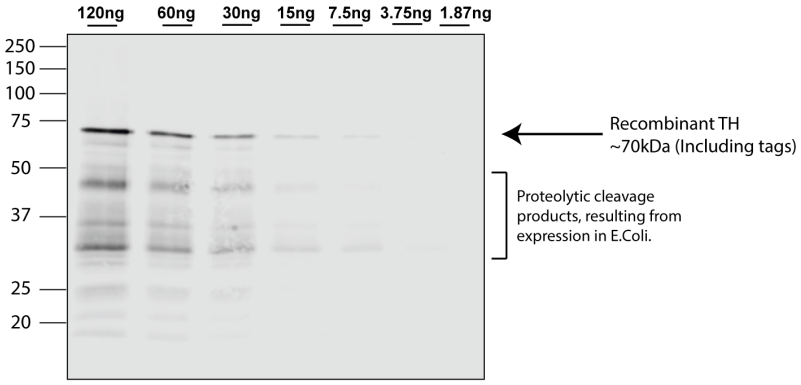

Supplementary Figure 1. Lower molecular weight bands in recombinant TH protein are proteolytic cleavage products resulting from prokaryotic expression of TH protein. Similar to lower molecular weight bands seen in Figure 2, proteolytic cleavage is evident in recombinant TH protein assayed by western blot.

Supplementary Figure 2

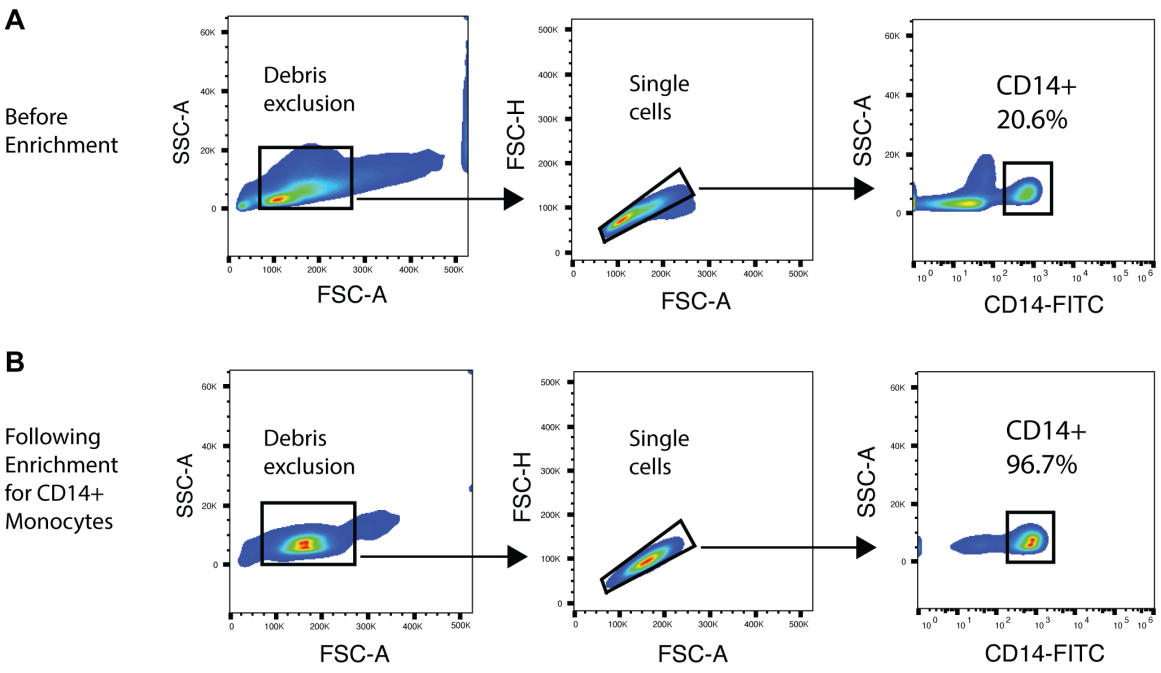

Supplementary Figure 2. Enrichment for CD14+ monocytes from total PBMCs. A) Total PBMCs isolated from healthy donor whole blood shows ~20% CD14+ monocytes as a fraction of total PBMCs. B) Following magnetic selection (see methods), a highly enriched population of monocytes consisting of greater than 95% CD14+ monocytes is available for downstream cell culture treatments.

Supplementary Table 1

Supplementary Table 1: Clinical data for Parkinson's disease patients								
Patient ID	Disease Duration (Years)	Sex	Age (Years)	H-Y	UPDRS Off	UPDRS On	Other Conditions	Medications
Parkinson's 149	7	M	71	2	33	--	None	Rytary, Ropinirole, Amantadine, Azilect, Apokyn
Parkinson's 150	9	M	50	2	--	26	None	Sinemet, Selegiline, Mirapex
Parkinson's 151	19	F	70	2	38	37	RLS	Sinemet, Pramipexole
Parkinson's 154	15	M	76	--	--	--	None	Asprin, Sinemet, Klonopin, Rasagilline, Rigotine
Parkinson's 155	9	M	85	3	--	25	HTN, T2D	Atorvastatin, Sinemet, Zetia, Losrtan, Metformin, Metoprolol, Flomax
Parkinson's 161	2	M	61	2	--	33	HTN	Amantadine, Sinemet, Atorvastatin, Losartan, Metoprolol, Omeprazol
Parkinson's 163	7	M	70	3	15	--	None	Sinemet, Amantadine, Flomax, Ropinirole
Parkinson's 164	4	F	67	--	17	--	None	Atorvastatin, Sinemet, Fluoxetine, Ganapentin, Losartan
Parkinson's 165	1	M	60	3	--	23	Arthritis	Sinemet, Amantadine, Celebrex, Sertraline, Trazadone
Parkinson's 166	3	F	67	3	--	--	None	Sinemet, Tylenol
Parkinson's 167	6	M	59	2	--	26	T2D	Sinemet, Asprin, Amlodipine, Metformin, Ibuprofen
Abbreviations: RLS (restless leg syndrome), HTN (hypertension), T2D (type 2 diabetes), H-Y (Hoen Yar), UPDRS (universal Parkinson's disease rating scale)								

Supplementary Table 1: Clinical data for Parkinson's disease patients. All PD patients and healthy control subjects were free from blood borne pathogens, viral/bacterial infections, had not been treated for infections within the preceding 21 days and were not taking blood thinners other than aspirin. Detailed medical histories for healthy control subjects were not available, other than those data presented. UPDRS Off represents Part 3 motor scores when subjects were not currently administered dopamine replenishment therapy (L-DOPA/Sinemet). UPDRS On represents Part 3 motor scores 30 minutes following dopamine replenishment therapy (L-DOPA/ Sinemet).